

1997

Photo-densitometry: radiograph digitization and algorithmic enhancement of x-ray images

Raghuram Madabushi
Iowa State University

Follow this and additional works at: <https://lib.dr.iastate.edu/rtd>

 Part of the [Computer Engineering Commons](#)

Recommended Citation

Madabushi, Raghuram, "Photo-densitometry: radiograph digitization and algorithmic enhancement of x-ray images" (1997).
Retrospective Theses and Dissertations. 243.
<https://lib.dr.iastate.edu/rtd/243>

This Thesis is brought to you for free and open access by the Iowa State University Capstones, Theses and Dissertations at Iowa State University Digital Repository. It has been accepted for inclusion in Retrospective Theses and Dissertations by an authorized administrator of Iowa State University Digital Repository. For more information, please contact digirep@iastate.edu.

**Photo-densitometry: Radiograph digitization and algorithmic
enhancement of x-ray images**

by

Raghuram Madabushi

A thesis submitted to the graduate faculty
in partial fulfillment of the requirements for the degree of
MASTER OF SCIENCE

Major: Computer Engineering

Major Professors: Charles Wright and Joseph N Gray

Iowa State University

Ames, Iowa

1997

Copyright © Raghuram Madabushi, 1997. All rights reserved.

Graduate College
Iowa State University

This is to certify that the Master's thesis of
Raghuram Madabushi
has met the thesis requirements of Iowa State University

Co-major Professor

Co-major Professor

For the Major Program

For the Graduate College

TABLE OF CONTENTS

ACKNOWLEDGMENTS		vii
1 INTRODUCTION		1
Scope of Research		3
2 BACKGROUND		5
X-ray Radiography		5
Digital Representation of X-ray Radiographs		8
Image Enhancement Techniques		11
Point Operations		11
Spatial Operations		13
Transform Operations		14
Available Systems for Radiographic Imaging and Processing		15
3 SYSTEM DESCRIPTION		17
Photo-densitometry		17
Image Acquisition and Digitization		23
Description		26
Algorithm		31
Calibration		32
Choice of Light Intensity		33
4 RESULTS		40
Field Runs		40

Weld Thickness Measurements	43
EPRI's Proposed Standard	44
Digitized ASTM Standard Radiographs	45
5 CONCLUSIONS AND FUTURE WORK	59
Future Work	61
REFERENCES	62

LIST OF FIGURES

Figure 3.1	Dynamic range of densities in an digitizer.	18
Figure 3.2	Digitized image of a aluminum step wedge with low illumination.	20
Figure 3.3	Grayscale versus density.	21
Figure 3.4	Digitized image of a aluminum step wedge with high illumination.	22
Figure 3.5	Grayscale versus density.	23
Figure 3.6	System for image acquisition and processing.	24
Figure 3.7	Calibration curves at different light intensities (expressed as a % of maximum).	27
Figure 3.8	Image of the standard calibration strip radiograph.	28
Figure 3.9	Image scaling.	30
Figure 3.10	Improper calibration curves.	34
Figure 3.11	Discontinuous composite image.	35
Figure 3.12	Calibration curve at 80% of maximum intensity.	36
Figure 3.13	Image of calibration radiograph at 80% of maximum intensity. .	37
Figure 3.14	Calibration curve at 55% of maximum intensity.	38
Figure 3.15	Image of calibration radiograph at 55% of maximum intensity. .	39
Figure 4.1	Image of air conditioner compressor part taken at an illumination of 80% of maximum.	41
Figure 4.2	Image of air conditioner compressor part taken at an illumination of 70% of maximum.	42

Figure 4.3	Image of air conditioner compressor part taken at an illumination of 60% of maximum.	43
Figure 4.4	Image of air conditioner compressor part taken at an illumination of 55% of maximum.	44
Figure 4.5	<i>Compositized</i> image, resulting from the image enhancement process.	45
Figure 4.6	<i>Composite</i> image with gray-scale window of 2389-3893.	46
Figure 4.7	<i>Composite</i> image with gray-scale window of 3072-4160.	47
Figure 4.8	<i>Composite</i> image with gray-scale window of 5415-7205.	48
Figure 4.9	<i>Composite</i> image with gray-scale window of 7214-8192.	49
Figure 4.10	Welding profile of a transmission casing.	50
Figure 4.11	Thickness versus gray-scale calibration.	51
Figure 4.12	Standard sample image.	52
Figure 4.13	Eaton transmission casing's image.	53
Figure 4.14	EPRI's proposed standard radiograph, under test.	54
Figure 4.15	Image of ASTM's standard radiograph showing shrinkage porosity.	55
Figure 4.16	Image of ASTM's standard radiograph showing sand and slag inclusions.	56
Figure 4.17	Composite image of penetrometer radiograph.	57
Figure 4.18	Composite image of penetrometer radiograph with min-max window of 2657-3459.	58

ACKNOWLEDGMENTS

I would like to thank the members of my committee, Dr. Joe Gray, Dr. Charles Wright, and Dr. Doug Jacobson; for all the help they provided throughout this work.

Though words don't do enough justice, let me acknowledge, especially, the contribution of Dr. Joe Gray, not only through the thick and thin of this work, but also for providing an environment of freedom, fun and support for me to learn. You have been an inspiration.

Important contributors I'm indebted to include Yew Tong, Clay, Pavan and of course Simon; I'd be happy if they had, even, half as much fun as I had working with them. Suchi, Vasan, Vijay and Sanjeev, thanks for being such great friends.

Thanks are due to Vasu for all that he's done for me.

This work was an outcome of the inspiration: Ranga, Chandra and Murali.

Lastly the unnamed, but as important, few who have helped me complete this thesis, but whom I have not explicitly named here.

1 INTRODUCTION

Industrial investigation of material structure and composition is an integral part of the manufacturing design flow. It is possible to evaluate these properties by both destructive and non-destructive means. Non-destructive evaluation of materials is attractive for obvious reasons and x-ray NDE (Non-Destructive Evaluation) is a well established discipline. X-ray images of materials (represented and stored in the form of radiographs) are capable of providing valuable information regarding the presence of material defects such as, voids, cracks and inclusions. A common medium used to store an x-ray image is the film or radiograph. This is an analog representation of the x-ray image, produced by the photographic effect. This grayscale representation of the material under investigation, when analyzed, is able to provide the necessary information regarding the presence of defects.

The human brain has the ability to recognize patterns and differentiate minute variations in the grayscales of the radiograph, so long as these variations are within a particular range. In order to overcome this limitation of the human visual mechanism and to facilitate the objectives of storage, processing and transmission, it is necessary to transform this representation of the x-ray image as a radiograph, into a digital form. This also helps to extract quantitative physical parameters from a digitized image, which is not possible with an analog image which is only good at providing a qualitative overview of an image.

This process of digitization transforms the grayscale analog radiographic image to a digital form, by first dividing the analog radiograph into a number of regions, pixels. In

the digitized image each pixel is assigned a value proportional to the optical density of the analog radiograph's pixel. This digital representation of the image will resemble its analog counterpart depending on the number of pixels present in the digitized image, and the number of steps used to represent the variations of grayscale in the radiograph. Though, ideally, it is desirable to have as many pixels and steps as possible, it becomes costly to incorporate a digitizer which has a very high resolution (spatial as well as step).

It is necessary to overcome these bottlenecks by using innovative processing techniques which will extract the necessary information from the digital image and let the investigator enhance distinctive features in the image which may be particularly useful. Various algorithms for processing these images exist, and are widely used in such varied fields as medical diagnosis to remote sensing. These image enhancement algorithms can be used to improve image qualities including noise suppression, edge detection and trend removal. This work involved a specific focus on x-ray digital imaging and the enhancement of such images to provide a low-cost flaw detection mechanism using low-end (8-bit) film digitizers.

Prime areas of application of the methodology developed include inspection of nuclear reactor shields for micro-cracks. X-ray images of such structures are stored in the form of radiographs, and the quantity of such hard-copy images is high. If there was available a means to store these radiographic images in digital form it will aid in the periodic archiving of such images, which is mandatory in such high risk applications as nuclear reactors.

Air gaps and depth of penetration of weld, when two materials are welded together are indicators of the strength of the welding. Using radiographic, non-intrusive imaging techniques, it is possible to calculate such parameters. Such techniques are sought after in areas like transmission casings in automobiles.

Apart from the ease of storage, the need for remote access and retrieval of such information makes digitization of the radiographs attractive. In order that there is

minimum loss of information when such a digitization process is employed, further image processing and enhancement techniques are necessary.

Scope of Research

There exists high-end film digitizers capable of providing a very high pixel resolution and spatial resolution. These are laser based systems and these digitizers use 12-16 bits. The quality of the images obtained are of a high degree. Further, the time involved in digitizing a radiograph is minimal (typical commercial systems take 1 minute to digitize a 14 by 17 inch radiograph). Such systems are expensive, but, there are applications which justify such costs.

On the other end, are the low cost systems, which make use of a 8-bit digitizer and still try to maintain as much information content as a high-end system. Since the number of radiographs that need to be digitized periodically, as part of government safety regulations, is large, it is necessary to find means to digitize radiographs using cost effective, low-end systems, without losing much information. However, such systems must be able to meet the performance standards requirements, which include the ability to cover a wide range of optical densities ranging from 0 to 4, and also to provide spatial resolution of the order of 35 to 50 microns.

It is necessary to devise new schemes for film digitization and manipulation, if we envisage using low-end, 8-bit digitizers and meet the quality standards of the high-end counterparts.

The purpose of this work was to provide a low-cost means to digitize x-ray radiographic films that can provide material compositional and structural information. This information retrieval was done in two phases. The first involved designing a means to digitize radiographs by illuminating them and storing the digitized result as a file. The second phase was to devise an algorithm that would provide image enhancement

techniques to overcome limitations imposed by the image display system and the 8-bit digitizer that is used.

It was necessary to provide means to circumvent problems of the dynamic range of visible image densities (and hence grayscales), when viewing an 8-bit image. Since our objective was to use an 8-bit image and still be able to capture information that would throw light on minute variations in the optical densities of the radiograph, it was necessary to first gather the information from a number of sources, by varying parameters that would change the visible optical densities and cover the entire range of densities. Then, upon processing this information, a representation medium was necessary to display only that much information at a time, which would retain the detail and let the investigator traverse the range of densities he wishes to view at a given time, and display only this range.

The issue of obtaining calibration standards for processing different grayscale images digitized at varying illumination intensities was addressed, which showed the possibilities of algorithm-induced perturbations in the final composite image, the reasons for their occurrence and ways to tackle them.

Description of the background necessary for obtaining digital images from radiographic films, necessary mechanism for arriving at an image enhancement algorithm and the theory behind the representation of images is presented in chapter 2. Chapter 3 presents the description of the system used to obtain such images and the algorithm that was developed for this work. This also includes the calibration schemes that were used for this photo-densitometer system. Chapter 4 illustrates the results of the field trials on typical real-world materials (including Aluminum and steel castings). The summary of this work is presented in chapter 5, along with suggestions for further investigation to improve the digitization and image enhancement techniques.

2 BACKGROUND

X-ray imaging helps in obtaining insightful information about the composition of a material in a non-destructive manner. It is necessary to process the information available from an x-ray radiograph, so that an investigator is able to visually inspect the material, and also this information must be ideally stored in some electronic means, so as to enable retrieval as well as transmission. The objectives of such a process involve understanding of 1) information about how an x-ray image is obtained and its characteristics, 2) method by which this x-ray image is transformed to be represented in a manner which will facilitate processing and storage.

This chapter discusses the background that has gone into all of the above objectives. First, the general x-ray imaging background will be presented, proceeding from which, a more general treatment of how an image is represented and the different methods of processing a digital image will be presented. Background for considering the various image enhancement algorithms and the image processing paradigm, in general, will be presented in this chapter.

X-ray Radiography

Non-Destructive Evaluation (NDE) of material imperfections is an intrinsic aspect of material characterization and inspection. Such methods of evaluation encompass a range of processes, extending from simple visual inspection to laser-based techniques. Radiography, ultrasound, eddy current, magnetic particles, and liquid penetration are

some of the widely used techniques [1].

Most of these techniques involves the excitation of a source of energy on the specimen under evaluation, observing the effects of this excitation and analyzing the results. Such investigation, which leave the material intact, provides useful information regarding the structural composition of the material, and hence, material defects (such as flaws including cracks, voids and changes in the material composition).

In the case of radiographic detection or evaluation, an x-ray beam is made incident on the material of interest, and the projections detected, thereby registering qualitative information of the object as well as the anomalies inherent in them. Ultrasonic techniques work by projecting an acoustic signal into a solid object, which is reflected when it reaches a flaw. Eddy current inspection involves supplying an electro-magnetic field to a metal specimen and observing the interaction.

Radiographic inspection NDE is inherently a visual inspection tool, in that, images and radiographs obtained upon x-ray excitation and registration on, generally, photographic films, are inspected by an individual to obtain information. This method does not require any physical contact with the object under investigation, and hence there are few restriction on the type of objects that can be subjected to such inspections. Interpretation of the data thus obtained is easy, with it being represented in an image form. The following will provide a background to the physical process of x-rays, their nature, interaction with material and the image detection techniques used. This will be useful in understanding the need to process the information obtained.

X-rays are high energy, ionizing, electro-magnetic radiation in the range of 1KeV to 1MeV [2]. Although they are invisible to human eyes they have a photographic action similar to visible light. There exists two methods to generate x-rays, the most common being the use of radio-isotopes or bremsstrahlung sources. These differ in the spectrum of radiations produced, with the former producing a single energy emission and the latter is typically produced by commercial x-ray machines, resulting in a broad spectrum of

energy. These are generated when electrons are created by a heated filament, and then accelerated to high energies and bombarded onto metal targets, the abrupt deceleration upon collision producing the x-rays. This study has used bremsstrahlung x-ray quanta, although the results of this work are not limited to these sources.

For material inspection, the x-ray beam is projected onto an object. The amount of absorption of the x-rays depends, among other things, on the density of the material. Hence, the object will scatter some photons and absorb some. The scattered photons and the photons not absorbed by the material fall on the detector, resulting in an image, which is characteristic of the object's material and composition. More photons reach the detector if the material region is thin, and vice-versa. Hence, in the film (which is the detector), the thicker material regions will have a lower film density and appear light in shade; with the thinner regions appearing dark.

A film is the most common industrial detector used, owing to, the high quality of image produced and the ability to lend itself to archival procedures. A radiograph is a photographic image produced upon the exposure of a film to the ionizing radiations which pass through the material under investigation. This film upon development, darkens with respect to the amount of incident radiation. A reaction occurs with the silver halide crystals within the film emulsion when the film is exposed to electro-magnetic radiations (light or x-rays) [3].

The levels of gray in such a radiograph can be characterized using optical density measurements using what is called a densitometer. Typical industrial radiographs have densities ranging from 0-5. The measurement of density is based on the intensity of the viewing light. Both the initial light intensity (I_0) and the transmitted light intensity (I_t) in the definition of film density are based on the light from illumination used to view the developed film. This intensity is not related to the aforementioned x-ray intensity. The optical density of the film [4] is defined by

$$D = \log_{10}(I_0/I_t)$$

The exposure (D) of the film is based on the speed of the film (s) and time (t) [5].

$$D = D_0(1 - e^{-s*I*t})$$

There exists an alternative to film/radiograph based imaging, *Real-Time Imaging*. This may be used in instances involving a large volume of materials under evaluation. Such a system consists of an image intensifier, a camera, and a monitor. The image intensifier, consisting of a phosphor screen, a light-to-electron screen behind it, a photo-multiplier, and an output screen, converts x-rays to visible light and increases the intensity of the image. The resulting image is then viewed using a camera subsequently connected to a monitor. For radiograph digitization this signal will then be fed to an imaging board on a computer. The digitization process electronically maps out the signal being received by the camera. The signal is converted to a numerical code that shows the intensity level of each pixel on a 0-255 scale, where black is equal to zero and white, to 255. This digital form can then be used to extract and process information about the image [6,7].

Digital Representation of X-ray Radiographs

As mentioned earlier, there exists a need to represent the x-ray radiograph in a digital form. X-ray image digitization proceeds in the following steps and has the following basic stages 1) the CCD Sensor, 2) Video pre-processing, 3) Analog video processing, 4) Video digitization and 5) Sync and power boards [8].

The light from the radiograph is brought into focus at the imaging plane of the CCD. An optical block filters out the IR component of light. In the CCD, integration time is defined as the duration for which charge is allowed to accumulate in the CCD charge sites. The amount of charge that is integrated in each pixel well is proportional

to the illumination received at each active pixel site on the CCD. Anti-blooming pulses during the horizontal and vertical blanking areas trigger anti-blooming gates that are an integral part of the active pixel. Blooming is the phenomenon in which a bright spot of light in the field of view of a video camera appears to be larger in size. This could result in unwanted artifact in the digitized image of the radiograph. Blooming occurs when a charge site, exposed to a very bright light, fills up with charge and then overflows to the neighboring charge site, causing a bright spot to appear larger in size. By deliberately decreasing the rate at which the charge well is filled beyond the half point, blooming is reduced.

During the vertical blanking interval (the interval during which the raster retracts to the first column of the charge matrix), the entire charge matrix that was integrated in the previous field (1/60 sec) is shifted to the opaque storage area of the CCD. This is accomplished by a series of pulses, each of which causes the charge matrix to shift down by one line. In the following field, the charges are transferred from the storage area of the CCD to on-chip serial shift registers and then sequentially to the detection nodes where they are made available as signal voltages. When one field is being read out from the storage area, the other field is being integrated in the imaging area of the CCD.

The low-level video signal voltage from the CCD is fed through a high-speed sample-and-hold amplifier, clamped (DC level shifted for black reference) and amplified before further video processing. It is in this section that the three channels of video corresponding to the three basic colors must be equalized, such that the contribution of these three individual channel's black reference are the same, before they can be multiplexed into a single channel of video. In order to accomplish this, two channels are provided with variable gain and offset; one channel (considered the reference channel) has fixed gain and offset. The two variable channels are adjusted by means of white balance and black balance potentiometers until all the three channels are properly matched.

The signal from the preprocessor stage is fed to the video processor which performs

the following functions related to the analog (RS-170) video:

(1) Gamma Correction: Gamma is a measure of the linearity of the camera's response to light. The CCD is inherently a linear device. The output signal is directly proportional to the scene illumination (or exposure). Doubling the exposure will double the output signal. But, the phosphors used to make the monitors are non-linear; typically, the phosphors have less brightness response for dark signals and more for bright signals. To compensate for this, the opposite kind of non-linearity is introduced in the video signal from the camera. The video processor adds gain for dark signals and reduces the gain for bright signals, such that the overall system (camera and monitor) produce a linear effect.

(2) Gain and Offset control: In order to tune the dynamic range of the camera to suit the application the gain of the camera can be varied. This helps in low-light applications. The increase in gain will also result in the increase of the noise.

(3) Sync Insertion: The composite sync signal is added to the output video signal to create the composite video signal.

(4) Video output driver: The video processor is directly capable of driving a 75 ohm co-axial cable.

The low level video signal from the pre-processor is clamped to a standard DC level and amplified on the sensor and video board before analog-to-digital conversion.

The output from the digitizer is a data stream of parallel 8 bit words. Several handshaking signals are also provided. This is translated by an image processor into frames of video by means of storing the video data into appropriate locations of a frame buffer, based on the information encoded in the handshaking signals. The number of pixels (charge collection sites) on the CCD are 755 (horizontal)×242 (vertical), with pseudo-interlacing resulting in an effective matrix of 755(H)×434(V).

Image Enhancement Techniques

Image enhancement refers to accentuation, or sharpening, of image features such as edges, boundaries, or contrast to make a graphic display more useful for display and analysis. The enhancement does not increase the inherent information content in the data. But it does increase the dynamic range of the chosen features so that they can be detected easily. Image enhancement includes gray level manipulation, contrast manipulation, noise reduction, edge crispening and sharpening, filtering, interpolation and magnification, pseudocoloring, and so on. The greatest difficulty in image enhancement is quantifying the criterion for enhancement. Therefore, a large number of image enhancement techniques are empirical and require interactive procedures to obtain satisfactory results. However image enhancement remains an important topic because of its usefulness in virtually all image processing applications [9].

There exist a relationship between the structure of images and 1) the problem of quantitative representation, 2) the effect of desired processing and/or unwanted distortion, and 3) the interaction of images with the human observer. They provide a framework in which we think about and perform our image processing tasks. We need to understand the relationship between the objective (physical) and the subjective (visual) aspects of many image processing tasks.

Some of the common image enhancement techniques available can be classified into, (1) Point operations, (2) Spatial operations, and (3) Transform operations.

Point Operations

Point operations are zero memory operations where a given gray level $u \in [0, L]$, is mapped into a gray level $v \in [0, L]$, according to a transformation

$$v = f(u)$$

Where input and output gray levels are distributed between $[0, L]$. Typically and in our case, $L = 255$.

Low-contrast images occur often due to poor or nonuniform lighting conditions or due to nonlinearity or small dynamic range of the imaging sensor. This transformation, called *contrast stretching* can be expressed as

$$v = \begin{cases} \alpha u, & 0 \leq u < a \\ \beta(u - a) + v_a, & a \leq u < b \\ \gamma(u - b) + v_b, & b \leq u < L \end{cases}$$

where, α , β and γ are the slopes which determine the relative contrast stretch. The parameters a and b (defining the valley between the peaks of the histogram) may be obtained by examining the histogram of the image. For example, the gray scale intervals where pixels occur most frequently would be stretched most to improve the overall visibility of a scene. The slope of the transformation is chosen greater than unity in the region of stretch.

A special case of contrast stretching where $\alpha = \beta = 0$ is called *clipping*. This is useful for noise reduction when the input signal is known to lie in the range $[a, b]$.

Thresholding is a special case of clipping where the output becomes binary. For example, a seemingly binary image, such as a printed page, does not give binary output when scanned because of sensor noise and background illumination variations. Thresholding is used to make such an image binary. This can be expressed as

$$v = \begin{cases} 0, & 0 \leq u < a \\ \alpha u, & a \leq u < b \\ L, & b \leq u < L \end{cases}$$

A *negative* image can be obtained by reverse scaling of the gray levels according to the transformation

$$v = L - u$$

Digital Negatives are useful in the display of medical images and in producing negative prints of images.

Intensity Level Slicing permits the segmentation of certain gray level regions from the rest of the image. This technique is useful when different features of an image are contained in different gray levels. We may express this gray-level window slicing as

$$v = \begin{cases} L, & a \leq u \leq b \\ 0, & \text{otherwise} \end{cases}$$

which fully illuminates the pixels lying in the interval $[a, b]$ and removes the background.

It may be necessary to compress the dynamic range of the image data, when it is very large. For example, the dynamic range of an image is so large that only a few pixels are visible. This dynamic range can be compressed via the logarithmic transform

$$v = c \log_{10}(1 + |u|)$$

where c is a scaling constant. This transformation enhances the small magnitude pixels compared to those pixels with large magnitudes.

In many applications it may be desired to compare two complicated images. A simple but powerful method is to align the two images and subtract them. The difference is then enhanced. This is called *Image Subtraction*.

Spatial Operations

Many image enhancement techniques are based on spatial operations performed on local neighborhoods of input pixel locations.

When each pixel is replaced by a weighted average of its neighborhood pixels, that is

$$\sum \sum_{(k,l) \in W} a(k,l)y(m-k,n-l)$$

where $y(m,n)$ and $v(m,n)$ are input and output images, respectively, W is a suitably chosen window, and $a(k,l)$ are the filter weights, it is called spatial averaging. An example of one such spatial averaging filter is one with equal weights, giving $a(k,l) = 1/N_w$, where N_w is the number of pixels in the window W .

Such spatial averaging is useful for noise smoothing, low-pass filtering, and sub-sampling of images.

To protect the edges from blurring while smoothing, a direction averaging filter can be useful. Spatial averages $v(m,n : \theta)$ are calculated in several directions as

$$v(m,n : \theta) = \frac{1}{N_\theta} \sum_{(k,l) \in W_\theta} y(m-k, n-l)$$

and a direction θ^* is found such that $|y(m,n) - v(m,n : \theta^*)|$ is minimum. Then

$$v(m,n) = v(m,n : \theta^*)$$

gives the desired results.

In *Median Filtering*, the input pixel is replaced by the median of the pixels contained in a window around the pixels, and the pixels are arranged in the window in increasing or decreasing order and picking the middle value. The advantage is that it can remove isolated lines or pixels while preserving spatial resolutions.

Transform Operations

In the transform operation enhancement techniques, zero-memory operations are performed on a transformed image followed by the inverse transformation. Starting with a transformed image $\mathbf{V} = v(k,l)$ as

$$\mathbf{V} = \mathbf{A}\mathbf{U}\mathbf{A}^T$$

where $\mathbf{U} = u(m,n)$ is the input image. Then the inverse transform of

$$v^*(k, l) = f(v(k, l))$$

gives the enhanced image as

$$U^* = A^{-1} V^* A^{T^{-1}}$$

Available Systems for Radiographic Imaging and Processing

Most systems available for an NDE inspector, do not provide a tool to manipulate the regions of interest in the image density ranges of 0 to 4.5. Though, there exists radiograph digitizers capable of providing a digital image which can capture the entire dynamic range of the typical radiographs, these incorporate 14 or higher bit digitizers, which makes them costly.

Video Contrast Enhancers:

These instruments provides real-time contrast expansion, shading correction, and inversion. The contrast enhancement function improves visibility of low contrast features by stretching a selectable portion of the input video's grayscale to fill a larger gray scale range at the output. Those portions of the grayscale not selected for stretching are compressed so that the overall video amplitude remains unchanged. Shading correction can improve an unevenly illuminated image by increasing or decreasing brightness in selected regions. The inversion function, by creating a negative image, can improve visibility of cracks, pits, scratches, and defects on highly reflective surfaces.

Capabilities of easily specifying a region of interest for manipulation seldom exist. It will be easier if one is able to qualitatively manipulate an image and see the results on a visual display. One way to do this would be to use high end digitizers which can provide good image resolution and contrast. But, the human eye has a fixed range of discerning the minute changes in the grayscales, and hence it is difficult to obtain information regarding material compositional variations. Hence, it would be easier to

provide a small range of viewable grayscales at a time, and make this range dynamic, providing the investigators with a GUI tool which will let them move across the range of grayscales, rather than providing him with a higher bit image with a lot of information at a time.

Film Digitizers:

Most film digitizer need to employ a scanning laser beam to measure film optical density (OD) one pixel at a time with high signal-to-noise ratios in order to obtain high resolutions and optical density resolutions. It will be more cost effective if we can incorporate a CCD camera as the image acquisition component, and still come up with techniques to extract as much (if not more) information as one would, if we use the above mentioned, commercially available digitizers.

Such systems do not have any dynamic capability to increase the range of optical densities they are capable of acquiring. We would have to have more than one such digitizer if we need information at higher densities. If however there was a means to dynamically specify such ranges, and have the system configure itself to change the illumination intensities, as appropriate to such densities, and digitize the radiographic image, it will be more cost effective and at the same time, will lend us with more information.

3 SYSTEM DESCRIPTION

Image quality enhancement in order to obtain more information from a digitized x-ray image is an important aspect in non-destructive evaluation of materials. This is used to view various material defects (flaws) which may not be visible if certain image processing techniques are not applied to salvage such information. A new algorithm and technique to do the aforementioned is presented in this chapter.

Photo-densitometry

An x-ray radiograph has regions of differing densities ranging from 0 to 5 (in typical applications), with the lower densities of the radiograph representing highly dense material regions and higher densities, the less dense regions. Material defects which have different densities from the parent material show up in the x-ray radiograph as regions of different gray-scales. Upon the digitization of this radiograph, one must be able to distinguish these flaws. If the difference in the grayscales of the defect region and the parent region are less than the gray-scale step size of the image, it will not be possible to distinguish between these two regions in the digitized image.

A digitized image is obtained from an x-ray radiograph by back-illuminating the radiograph and digitizing it. A digitized gray-scale image of an x-ray radiograph could be anything ranging from 8 to 24 bits (or higher). This describes the number of bits available for encoding each of the pixels during digitization. Hence an 8-bit gray-scale image has 2^8 (256) gray-scale levels. A 24-bit image is able to represent an image in

detail, better than an 8-bit image because one is able to distinguish between finer gray-scale levels in the 24-bit image. Hence the number of bits used for digitization decides the amount of detail that is captured in the digitized image.

The camera used for digitization has a fixed dynamic range. This is the range of optical densities the camera is capable of distinguishing in the radiograph being digitized, as a result of variations in the range of light intensities reaching the camera. Hence, depending on this dynamic range, there is a limitation on the region of optical densities one wishes to register, in the digital image.

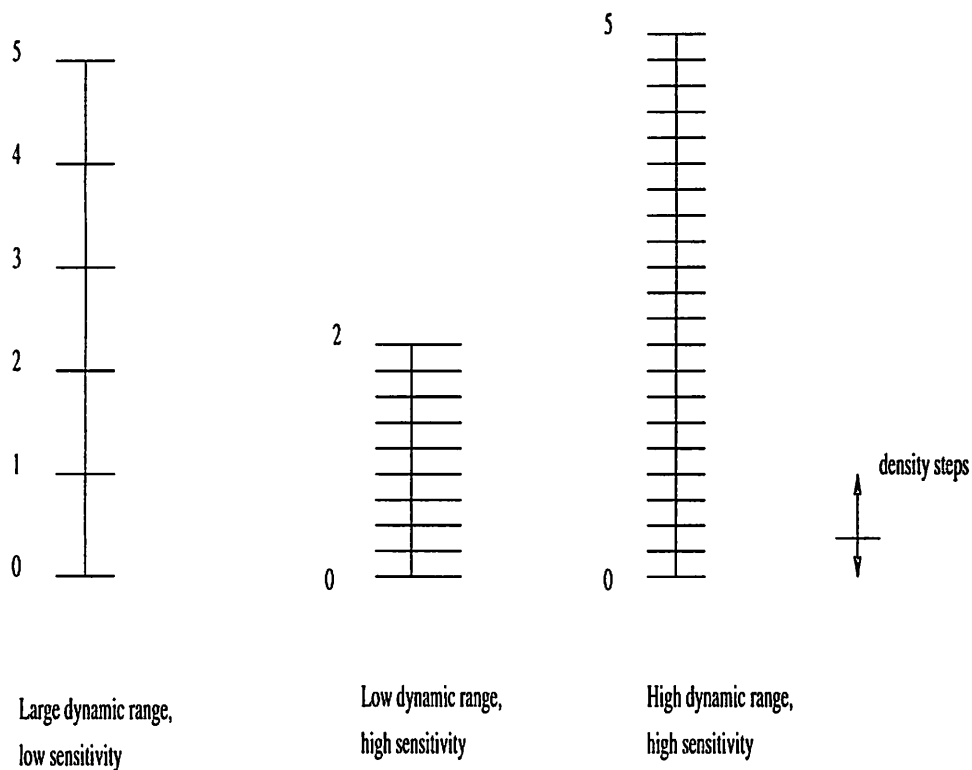


Figure 3.1 Dynamic range of densities in a digitizer.

Figure 3.1 shows these limitations of a camera used for digitization. It is possible to have a camera capable of covering a wide range of optical densities (0 through 5). This is called the dynamic range of the camera, which gives you a measure of the ability of the camera to register variations in the optical density over a wide range. On the

other hand, such cameras may have low sensitivity. Sensitivity is a measure of the ability of the camera to capture minute variations in the optical densities. The steps within which the camera is able to distinguish between densities is called the step size. Typically, a highly sensitive camera only has a small dynamic range. We must be able to capture these minute variations, and also be able to traverse a wide dynamic range of densities. Such a scenario is also presented in Figure 3.1. The digitizer must be able to register minute variations in the optical densities and distinguish between them. An optical density variation of 0.001 should be registered in the digitized image. This can be accomplished only if the digitizer has available high number of bits (16-18) such that it is sensitive enough to divide the available light intensity range into small steps.

An 8-bit camera has available 256 levels to encode the range of optical densities. At the same time 16-bit camera has 65536 levels available to encode the range of optical densities. Sensitivity of an 8-bit camera, hence is less compared to a 16-bit camera. Further there are available high-end cameras which have a wide dynamic range. A low cost CCD camera has a limited dynamic range (typically in steps of 1) of coverable densities. One method to overcome this limitation is to have more than one digital image of the same radiograph with each digital image covering a specific range of densities. Evidently, this will result in a number of images necessary to be stored, for one radiograph.

Since we are illuminating the radiograph, it is necessary to ensure that the light box is capable of providing enough light for the higher optical densities to register valid encoding.

Figures 3.2, 3.3, 3.3 and 3.5, show typical digitized radiographic images at two different illumination intensities. It can be seen from these images that, in the first image (Figure 3.1), information is available about the range of densities between 0.5 to 1.4. All regions with optical densities greater than 1.4 result in a fully dark pixel (gray scale of approximately 0). Hence this particular image has not been able to register information about regions with densities above 1.4. The second image (Figure 3.4) is one taken at a

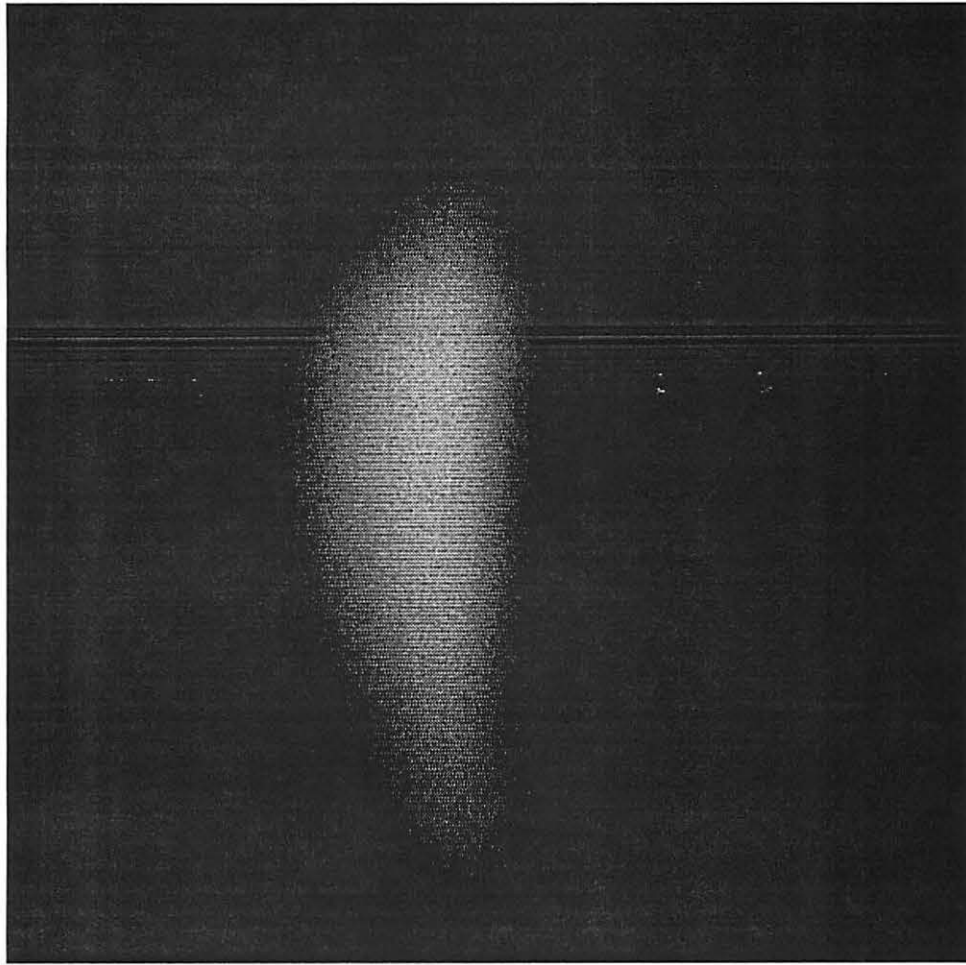


Figure 3.2 Digitized image of a aluminum step wedge with low illumination.

different light intensity and it can be seen that this particular image has been capable of capturing information about regions with optical densities lying in the range 2 to 2.9. All regions with densities less than 2.0 has resulted in a fully bright, flushed grayscale of 255. We can gather no information about regions with optical densities less than 2.0 from this (Figure 3.5) image.

We must hence find a means to be able to capture information about the entire dynamic range of optical densities in one digital image.

Photo-densitometry is an innovative way to overcome these limitations of the digitization process. In this method, different digital images are taken, of the x-ray radiograph,

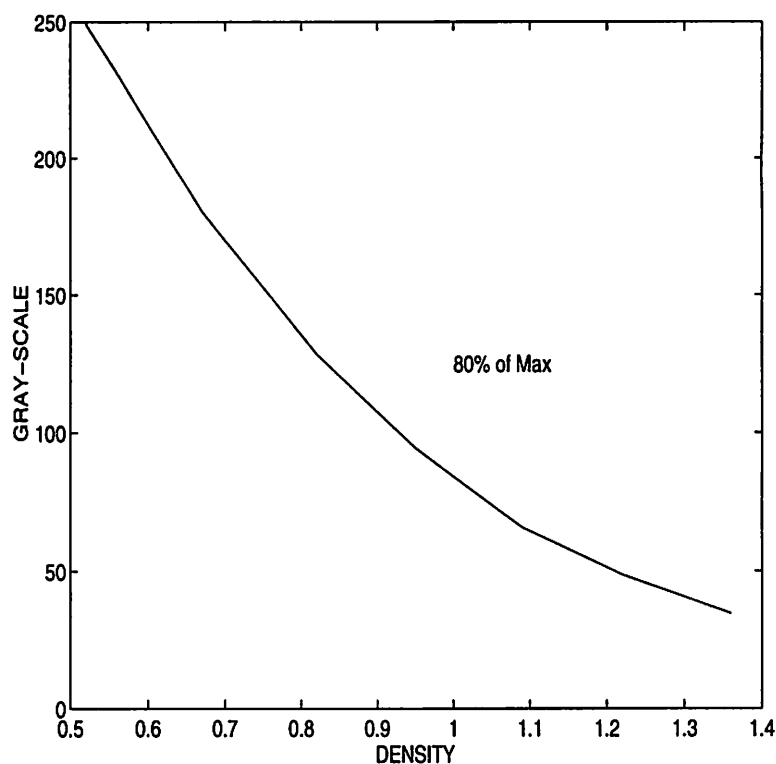


Figure 3.3 Grayscale versus density.

at different light illumination intensities. This results in digital gray-scale images of the same radiograph. But, each of these digitized images may contain information which could not be registered by other images due to the reasons mentioned above. Each of these individual images are 8-bit images, but, because of the corresponding illumination, they are able to capture film densities from 0 to 4, with each image covering a specific film density range.

The Photo-densitometer is able to take in these different digital gray-scale images and obtain one composite image. By specifying the region of gray-scales (or optical densities) which need to be viewed, the composite image is processed to display the region of interest, by scaling it to the entire 8-bits. Hence, there is no loss of information due to the limitation of the digitization process and one can scroll through the entire range of densities, viewing minute nuances in the gray-scales which throws light on the

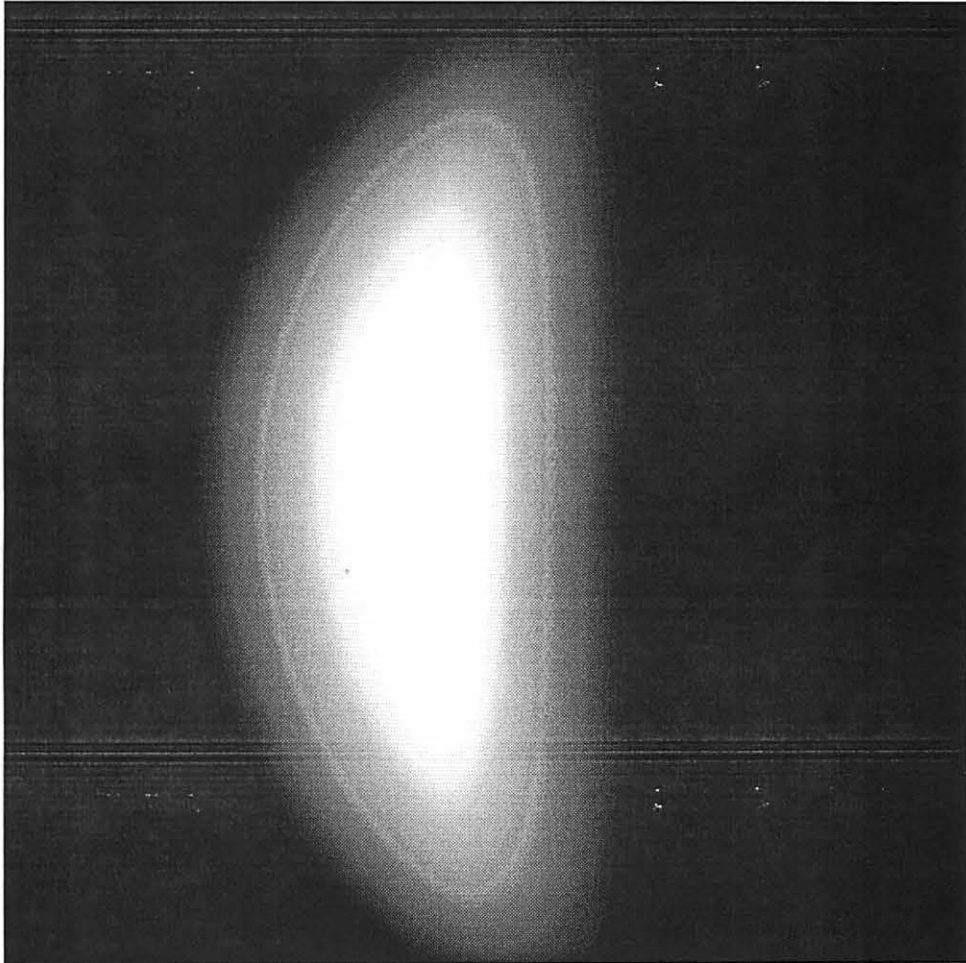


Figure 3.4 Digitized image of a aluminum step wedge with high illumination.

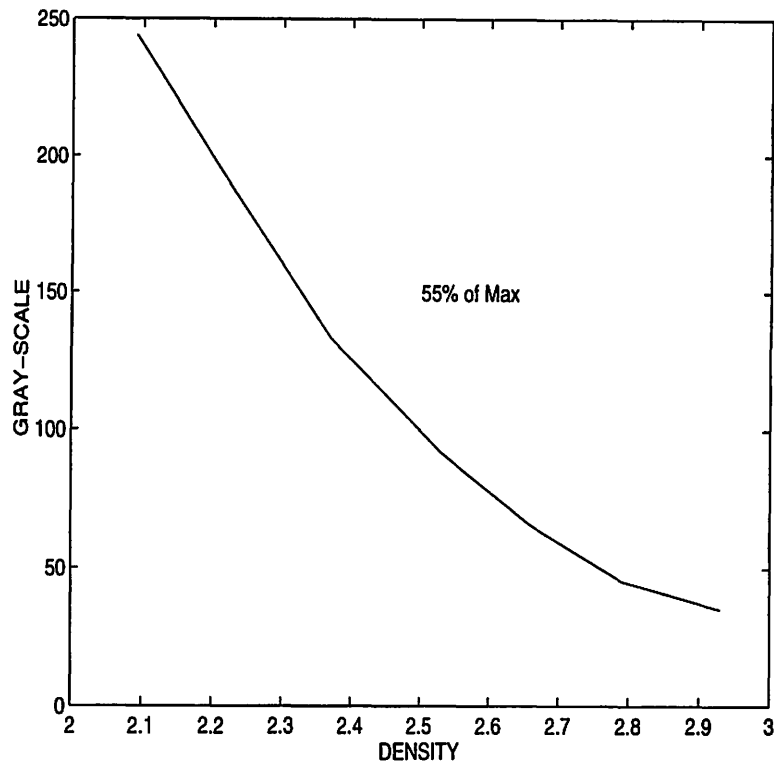


Figure 3.5 Grayscale versus density.

composition of the material and come up with insightful information about defects, which are not visible under normal imaging techniques.

Image Acquisition and Digitization

In order to digitally process an image it is necessary to record the image as a file and store it. Most film digitizers available now are laser based digitizers which are costly. A more cost effective way to digitize an x-ray radiograph would be to use a video camera, a frame grabber and a light-box for back-illuminating the radiograph (Figure 3.2).

A variety of cameras are available which are capable of acquiring an image and translating it into a composite video signal. Examples among these include the CCD (Charge Coupled Device) and CID (Charge Induced Device).

In terms of electronics a CCD can be described as a series of parallel plate capacitors

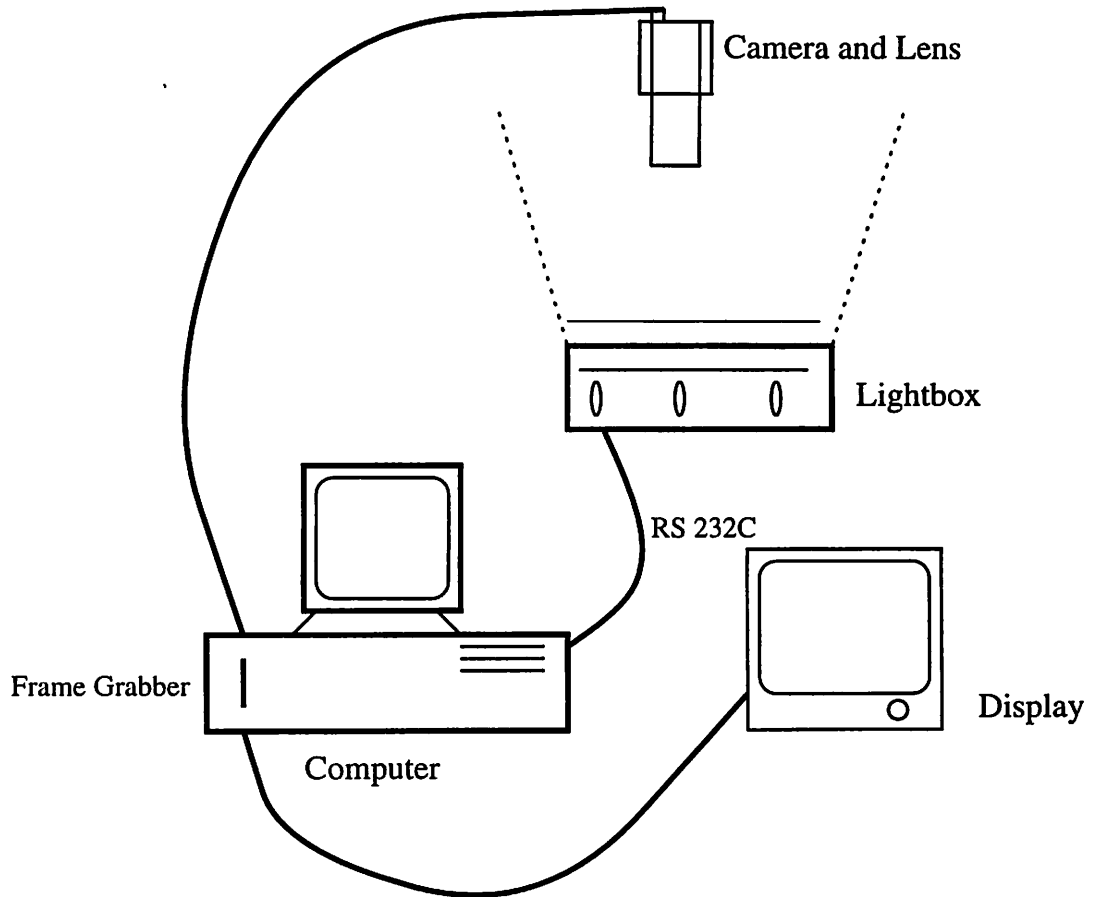


Figure 3.6 System for image acquisition and processing.

which store charge. The charge is optically generated by the absorption of photons which are converted to electron hole pairs in the same manner as a typical photo-diode sensor. The major difference, however, being that this diode is operated in the integrating mode than the conducting mode. That is, instead of reverse biasing the diode and constantly sensing the current increase caused by photons, a CCD photo-element senses the change in voltage induced by the collection of charge in a short period of integration. The period of integration must be shorter than around 100 ms due to the fact that the CCD has a temporary space charge depletion layer created by a pulse of negative bias on the diode. This effect is governed by the equation $CV=Q$. That is, for a given capacitance, a sensed charge will provide a corresponding voltage. The charge generated is then transferred into a shift register which is known as a CCD. The charge is then transferred by a series of pass or transfer gates. The camera operates the CCD sensor by providing the necessary biasing and clocking information to run the charge storage capacitors in the correct sequence. The signal charge is converted to a voltage by the sensor which is then amplified and conditioned by the camera.

The frame grabber acquires the composite video signal and converts a single frame into a digital form. The frame is broken down into a number of pixels with typically there being 640×480 (307200) pixels. Each pixel takes a gray scale value from 0 to 256 (if it is an 8-bit camera). Frame averaging is employed to suppress noise and also the light intensity fluctuations due to line voltage variations.

The light-box used for back illuminating the radiograph helps in improving the contrast. Uniform illumination must be ensured so that the light-box does not induce additional artifacts. Additionally variable light intensity control is necessary for obtaining images at different intensities.

The digitization equipment used for this work included a Data Translation Digitization Board, a COHU High Performance CCD Camera and a Light-box from S & S X-Ray Products Inc., fitted with three No. 2 Super Flood EBV bulbs. The light-box

was capable of going up to a brightness of 13000 foot-candles. Further, in order to obtain a good range of view of the image, an AF Nikkor 28-85 mm, 1:3.5-4.5 f-stop lens, was used for this work.

Description

First the four gray-scale images are read. An image is represented as a two-dimensional $M \times N$ array of non-negative integers $f(x,y)$, where $1 < x < M$ and $1 < y < N$ are coordinates of structures in the image. The image segment represented by the coordinates (x,y) is called a picture element or gray level (gray-scale). The gray level ranges from 0 to 255. This gray level represents the optical density of the square area of the film [3].

A two-dimensional radiologic image has a size of $M \times N \times k$ bits, where 2^k equals the gray level range. In our particular case, we consider a $640 \times 480 \times 8$ bits image.

A radiograph with an optical density of 0 will be very transparent allowing considerable amount of light to pass through it. This will cause a gray-scale of 255 to be registered. A radiograph with an optical density of 4.0, on the other hand will register a gray-scale of 0 and allow less light to pass through.

The first step in the algorithm involves the conversion from the gray-scale value of each pixel to the corresponding optical density value. The optical densities of the radiograph will be used for manipulation. This is so because, the optical density of a pixel is fixed for a radiograph, whereas the gray-scale depends on the intensity of light illuminating the radiograph.

This conversion from gray-scale to optical density is accomplished by the algorithm using the generic look-up table approach. For this look-up table, the standard values of gray-scales corresponding to optical densities under a given illumination is first recorded under similar environments. This enables us to obtain calibration curves for each light-box intensity, with curves representing the optical density for a given gray-scale. It

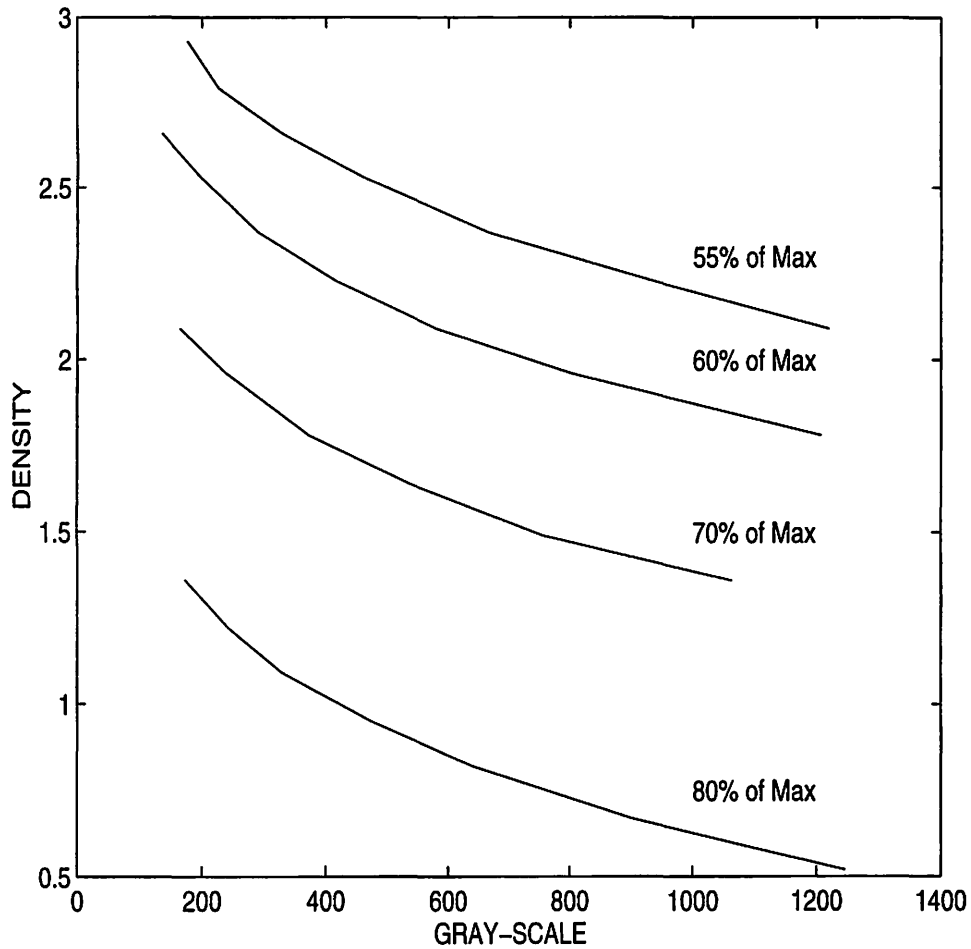


Figure 3.7 Calibration curves at different light intensities (expressed as a % of maximum).

was observed that the plot of gray-scale and optical densities obeyed an exponential relationship, and hence a polynomial fit to these curves will provide an equation which can be used as a standard for converting from gray-scales to optical densities for a given light-box illumination intensity.

A calibration strip with known optical densities, traceable to NIST, was used for this calibration step. The calibration curves along with the calibration radiographic strip are given in the Figures 3.7 and 3.8.

We now have four arrays containing the optical densities of the individual pixels of the

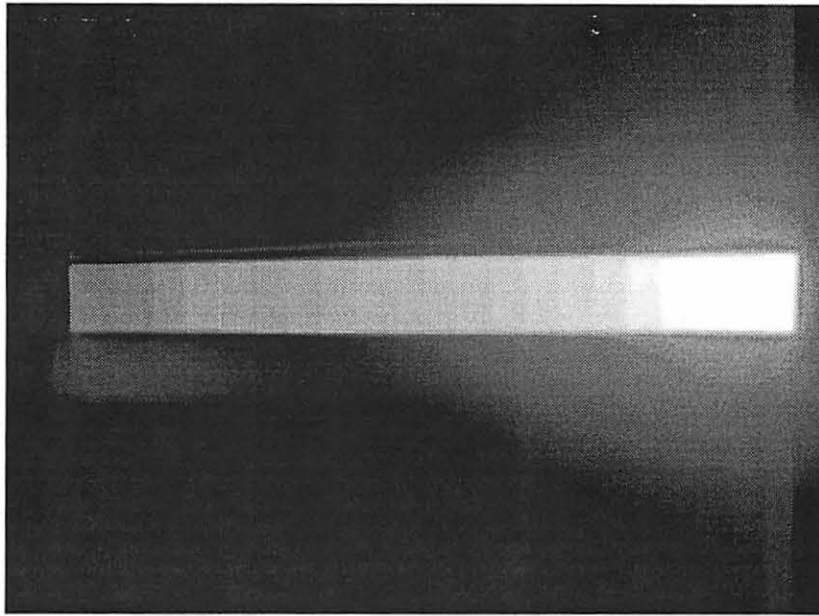


Figure 3.8 Image of the standard calibration strip radiograph.

image. Since these four images are of the same radiograph taken at four different light intensities, the optical densities which were saturated in the first image are represented in the second image and so on. Hence, the information regarding the entire optical density range is available, albeit as four different images.

The next step in the algorithm is to find a means to obtain an image which will have all the optical density information and represent it in a single file. This is referred to as *image compositization*. The algorithm proceeds to perform image compositization in the following manner. We proceed pixel by pixel and traverse through the entire image. Further, we proceed from image-1 through image-4 (with each of these images corresponding to a light intensity of a percentage of the maximum), considering one image at a time.

The first pixel of the first image is considered. If the optical density of this pixel is lesser than a specific critical optical density (with respect to this particular illumination intensity), we use the next image in line to obtain the correct optical density value. If, further, the optical density still remains lesser than a specific critical optical density

(with respect to this particular illumination intensity), we move over to the next image in line and obtain the correct optical density.

Once, for a particular pixel, we have obtained the correct optical density, by traversing from one image to another, we proceed to the succeeding pixel and perform the same above procedure to obtain the correct optical density value. At the end of this traversal through the digital image, pixel by pixel, and registering the actual optical density of the radiograph, we are left with an array containing the actual optical densities of the entire radiograph.

Once the user specifies the range of optical densities he wishes to view (done by specifying the minimum and maximum optical densities), all pixels containing optical density values lesser than the minimum specified value are made equal to the minimum optical density; on the other hand, all actual optical densities of pixels of the image having an optical density greater than the specified maximum are made equal to the maximum. Though, by doing so, we are losing information that may be present in the pixels which have optical densities lesser than the minimum (or greater than the maximum) and thereby ignoring flaws that might be present in the material, the rationale behind doing so is to provide the user with a small window in the density spectrum of the image and let him view the flaws that may be present inside this small window. After which one can move this proverbial window to view another set of optical densities.

All the pixels having optical densities between the minimum and maximum specified value are the pixels of interest and as much information as possible must be gleaned from this and provided for display. We have available 8-bits for display at a time. Hence, the algorithm scales the optical densities to this range, converts it to gray-scale and displays the compositized image. This is shown in Figure3.9.

What this image optical density scaling does is to map the density variations between the minimum and maximum to a range of 256 gray-scale values. Thus, we have reduced the lost information owing to the restriction of both the 8-bit camera/digitizer and the

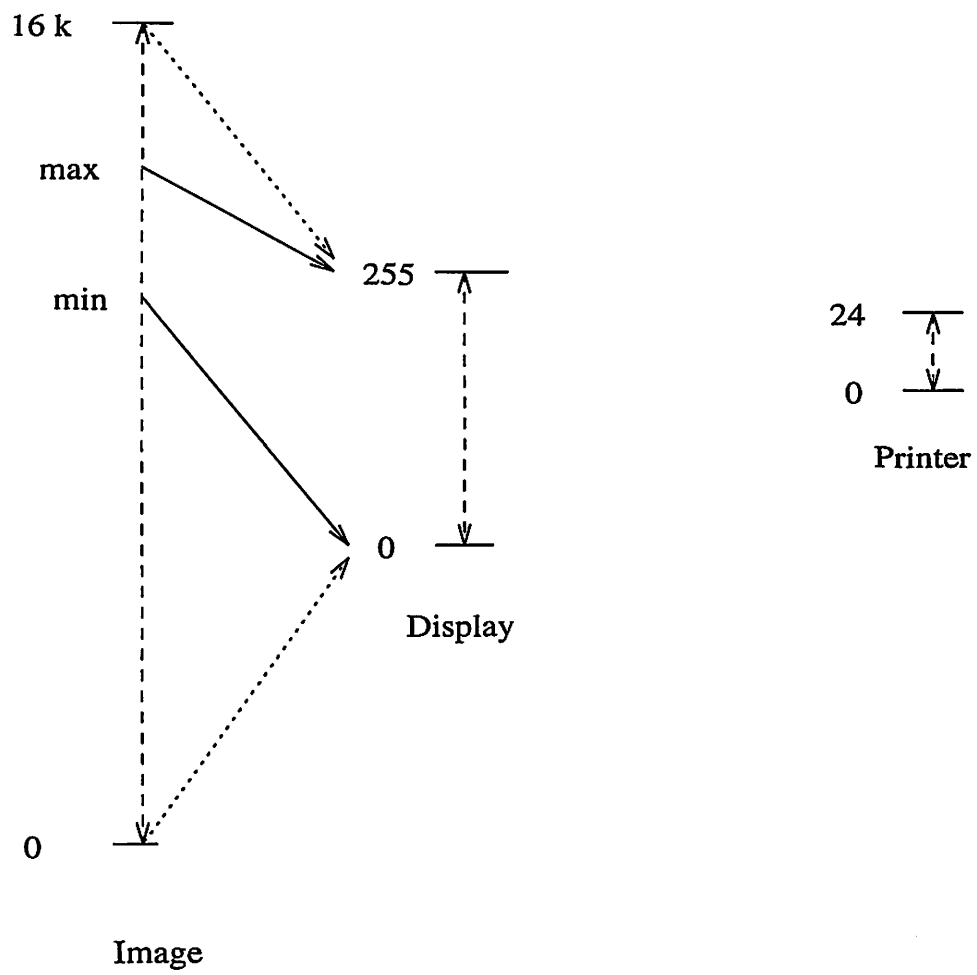


Figure 3.9 Image scaling.

8-bit display. Even minute variations in the optical density of the radiograph is now picked up by the algorithm and scaled up to a level where it becomes obvious to the investigator.

Algorithm

The algorithm for obtaining a composite image from four different images is given below -

begin:

Read the 4 Image files into 4 arrays:

ImageArray1 = Image at 80 % of maximum intensity

ImageArray2 = Image at 70 % of maximum intensity

ImageArray3 = Image at 60 % of maximum intensity

ImageArray4 = Image at 55 % of maximum intensity

Convert the gray-scale values of the pixels of each of the images into corresponding optical density values using the generic look-up table approach and store in separate arrays:

$$Dens1 = -0.418515 \log [ImageArray1] + 3.27845$$

$$Dens2 = -0.418983 \log [ImageArray2] + 3.9786$$

$$Dens3 = -0.359767 \log [ImageArray3] + 4.08223$$

$$Dens4 = -0.394983 \log [ImageArray4] + 4.62595$$

Perform Image compositization:

if (*Dens1* > 1.4)

 if (*Dens2* > 1.87)

 if (*Dens3* > 2.29)

$$CompositeDens = Dens4$$

 else

```

      CompositeDens = Dens3
    else
      CompositeDens = Dens2
    else
      CompositeDens = Dens1
Scale the image based on the minimum and maximum selected by the user:
CompositeImage = (-2048.0 (CompositeDens)) + 8192.0;
if(CompositeImage < minimum)
  CompositeImage = minimum
if(CompositeImage > maximum)
  CompositeImage = maximum
if(CompositeImage > minimum or CompositeImage < maximum)
  FinalImage = ((CompositeImage - minimum) \ (maximum - minimum)) × 255.0
Display FinalImage, the image scaled to the region of interest.
end.

```

The above terms represent individual pixels, and one must traverse though the entire image, and perform the above manipulation for each of these pixels.

Calibration

In order to convert the gray-scale image to an optical density image, a standard calibration strip radiograph, who's optical densities are known, is necessary.

For a given illumination of the light-box intensity, we need to calculate the gray-scale values of the known optical densities. A typical plot of the gray-scale versus the optical density is shown in Figure 3.6. These curves are for light intensities expressed as a percentage of the maximum. These calibration curves will be used to obtain the relationship between the gray-scale value obtained by the digitizer and the actual optical

density of the radiograph. An exponential best fit to these curves provides us with an exponential equation which can be used by the lookup table for conversion. Since we need to eliminate noise, we accumulate more than one frame and hence the gray-scale values range from 0 to 1275 for each image. It is necessary to maintain similar light conditions during calibration, as would exist during the actual process of image acquisition, so that we are able to convert accurately the optical densities of the radiograph.

Choice of Light Intensity

This is one of the crucial decisions one needs to take with respect to acquisition and calibration. Improper choice of calibration curves as shown in Figure 3.10 could lead to discontinuities in the composite image (shown in Figure 3.11).

The algorithm is as such that, when moving from pixel to pixel in an image, if the density is greater than the critical maximum of this particular curve, control should move to the next curve (and hence image). The choice of this critical maximum becomes very crucial.

Consider the first calibration curve, *curve1*, as shown in Figure 3.12. For an image taken at this light intensity, all optical densities greater than 1.0 will result in a gray-scale in the region where it is fully dark (gray-scales less than 40). Any artifact with matching densities (around 1.0) will not be visible in this particular image. But looking at the next curve, *curve2*, it is evident that optical densities close to and above 1.0, result in gray-scales in the vicinity of 200 (Figure 3.14 and 3.15).

An important aspect of discontinuity is that, this transition from one image to another must be smooth and continuous. Ideally, the choice of the calibration curves should be such that, the maximum correctly distinguishable optical density for *curve1* should also be the minimum correctly distinguishable optical density for *curve2* and so on.

What this continuity ensures is that, when, in the radiograph, there is a smooth transition of optical densities from 0.8 to 1.2, the pixels having densities of 1.0 and less

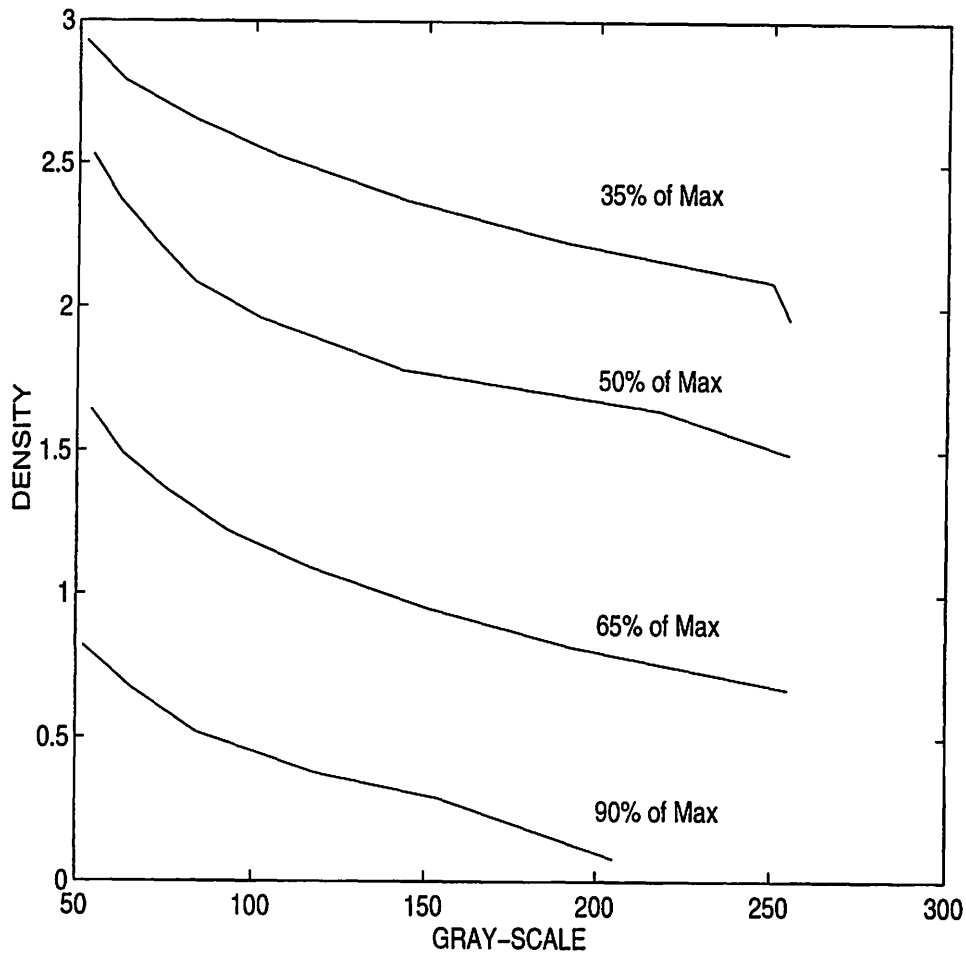


Figure 3.10 Improper calibration curves.

will be obtained from the first image, and for any optical density greater than 1.0, it will be obtained from the next image. Since for the first curve, any gray-scales less than 40 results in an erroneous interpretation of the optical density, we move over to the next curve to obtain the correct optical density. If there was a discontinuity, there will exist pixels having densities above 1.0, because of which the first curve will not be used to calibrate this pixel. But, since the minimum correctly identifiable optical density for the next curve is around 1.3 (owing to the discontinuity), all densities above 1.0 and less than 1.3 will be erroneously decoded.

An overlap of correctly identifiable densities and gray-scales must exist when choosing

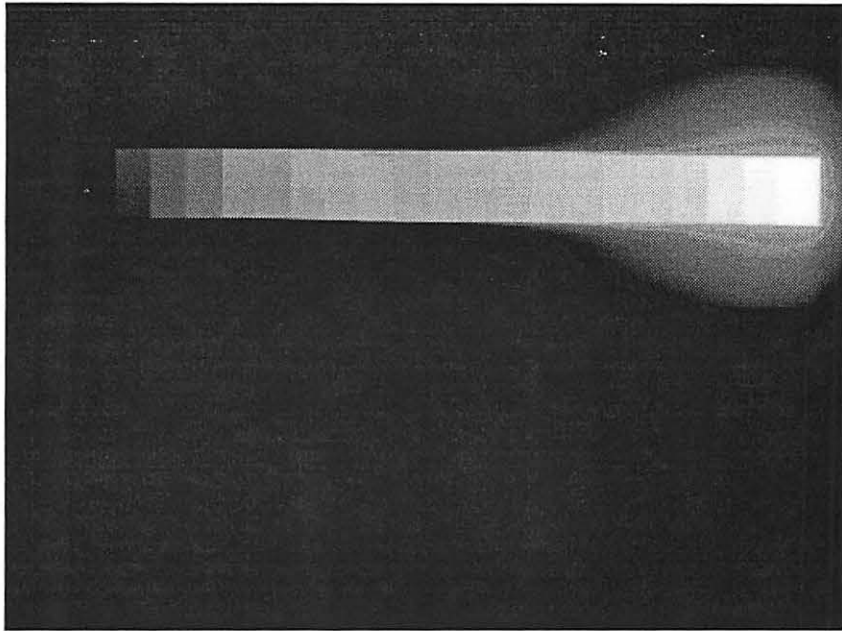


Figure 3.11 Discontinuous composite image.

the calibration curves. On the other hand, the curves should not be over cramped such that it requires a number of curves to decode a small range of densities.

The calibration curve equations used are given below for different curves -

curve1 at 80 % of maximum light intensity :

$$\text{density} = - 0.418515 \log [\text{grey-scale}] + 3.27845$$

curve2 at 70 % of maximum light intensity :

$$\text{density} = - 0.418983 \log [\text{grey-scale}] + 3.9786$$

curve3 at 60 % of maximum light intensity :

$$\text{density} = - 0.359767 \log [\text{grey-scale}] + 4.08223$$

curve4 at 55 % of maximum light intensity :

$$\text{density} = - 0.394983 \log [\text{grey-scale}] + 4.62595$$

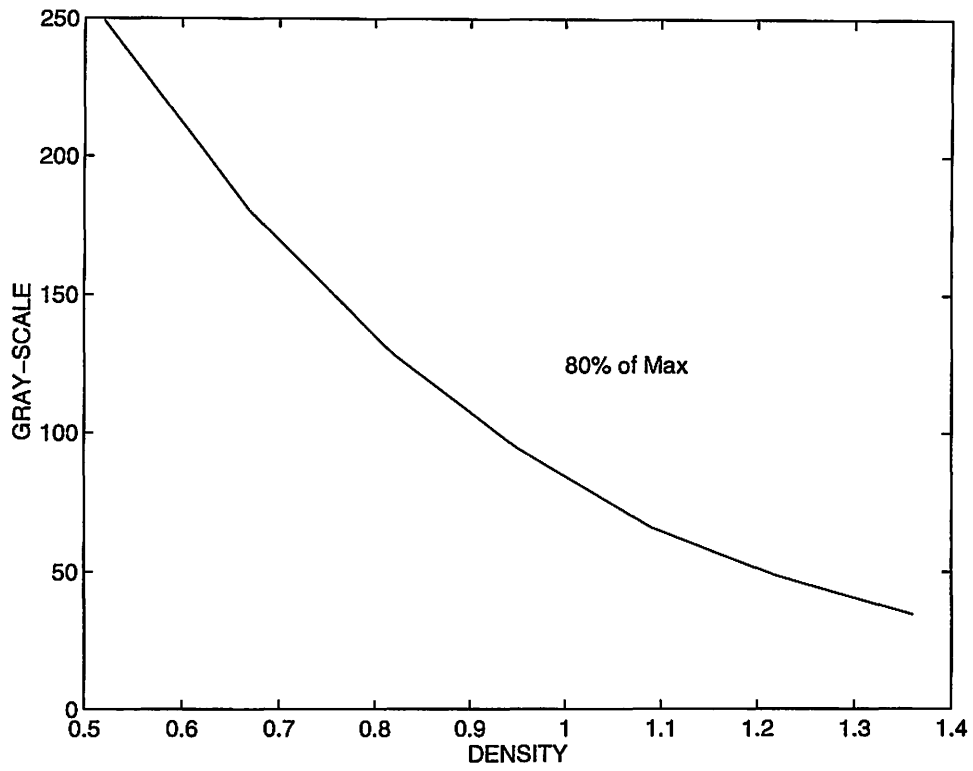


Figure 3.12 Calibration curve at 80% of maximum intensity.

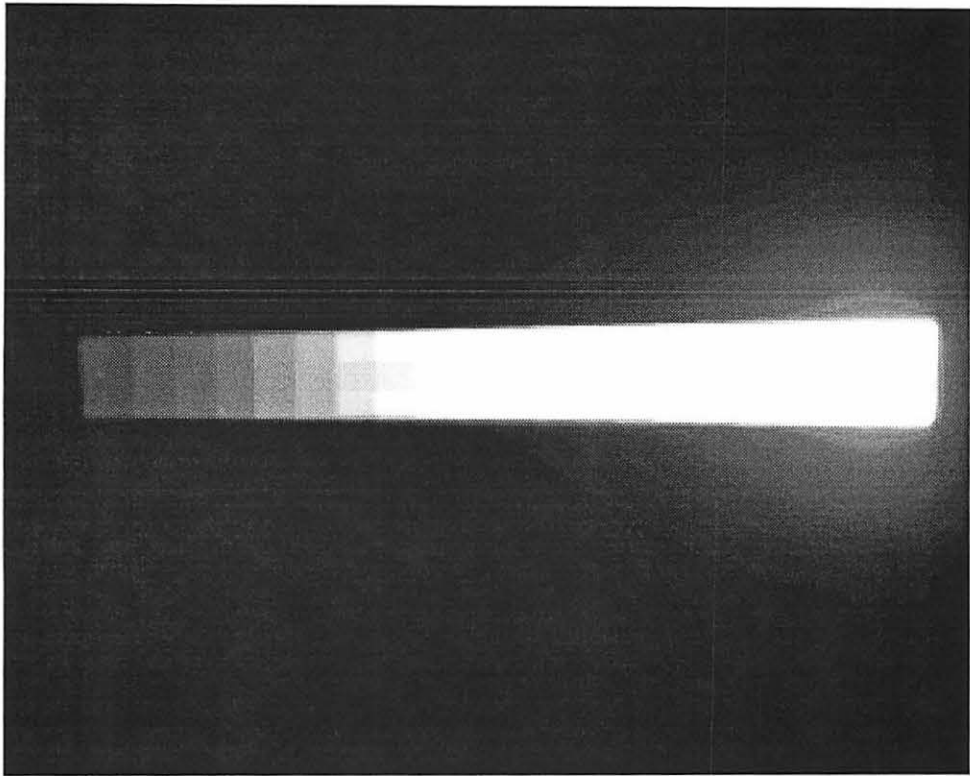


Figure 3.13 Image of calibration radiograph at 80% of maximum intensity.

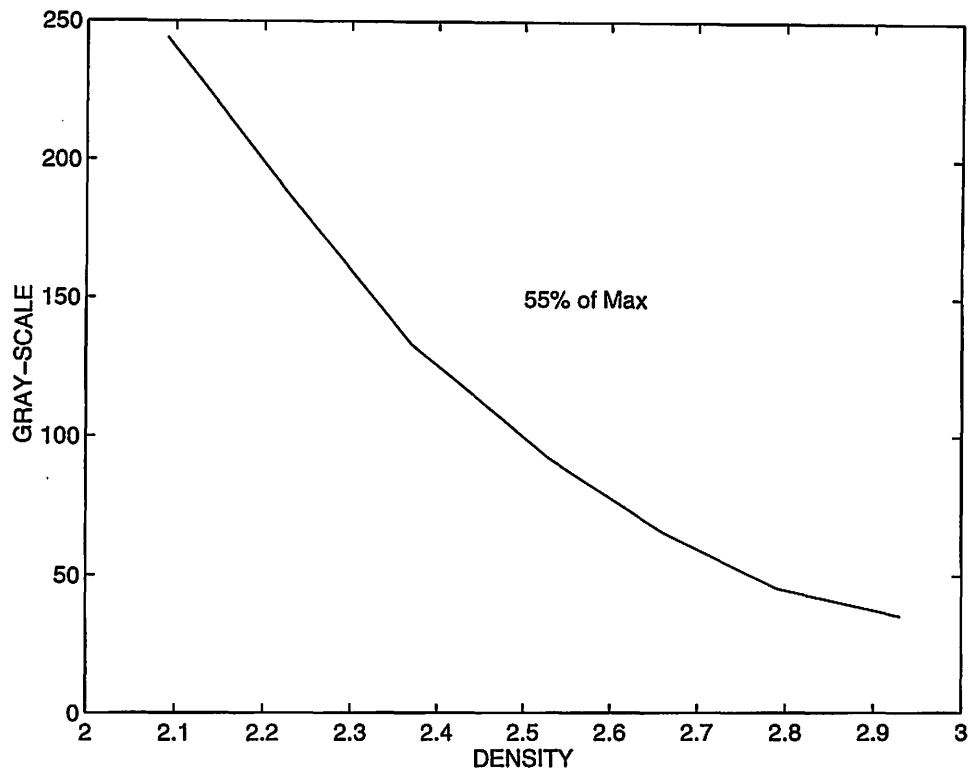


Figure 3.14 Calibration curve at 55% of maximum intensity.

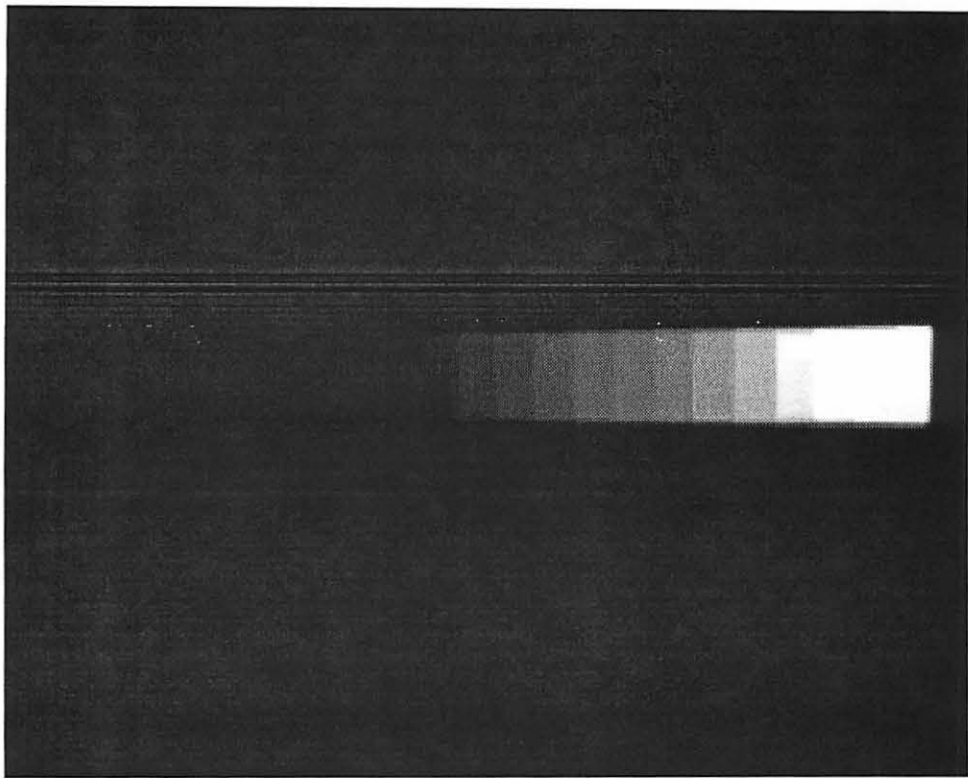


Figure 3.15 Image of calibration radiograph at 55% of maximum intensity.

4 RESULTS

Image enhancement is an important aspect of NDE, the first step in this process digitization of radiographs for both storage and information extraction. As was seen earlier, there are three stages involved in this scheme. First, is to obtain the x-ray radiograph of the object under investigation. Second, is to convert the formal representation of this x-ray radiograph into a form allow image processing. This involves digitization of the x-ray radiograph. Third, is to apply image processing and enhancement algorithms to obtain the information regarding defects and flaws in the material. This should result in an image which accentuates the flaws present in the material, for the investigator to visually detect them.

Field Runs

Figure 4.1 shows the image of a typical part, in this case an aluminum casting taken at a light intensity illumination of 80 % of maximum. Evident from this image, and as was discussed earlier, is that the region within an image density range of 0 to 1.5 is only manifest and visible. All densities above this maximum density of 1.5 results in a gray-scale of 0.

Figure 4.2 shows the same part's radiograph digitized under an illumination of 70% of maximum light intensity. This image shows that all densities of less than 1.5 results in a gray-scale of 255 and all pixels having an image density of greater than 2.0 results in a gray-scale of 0.

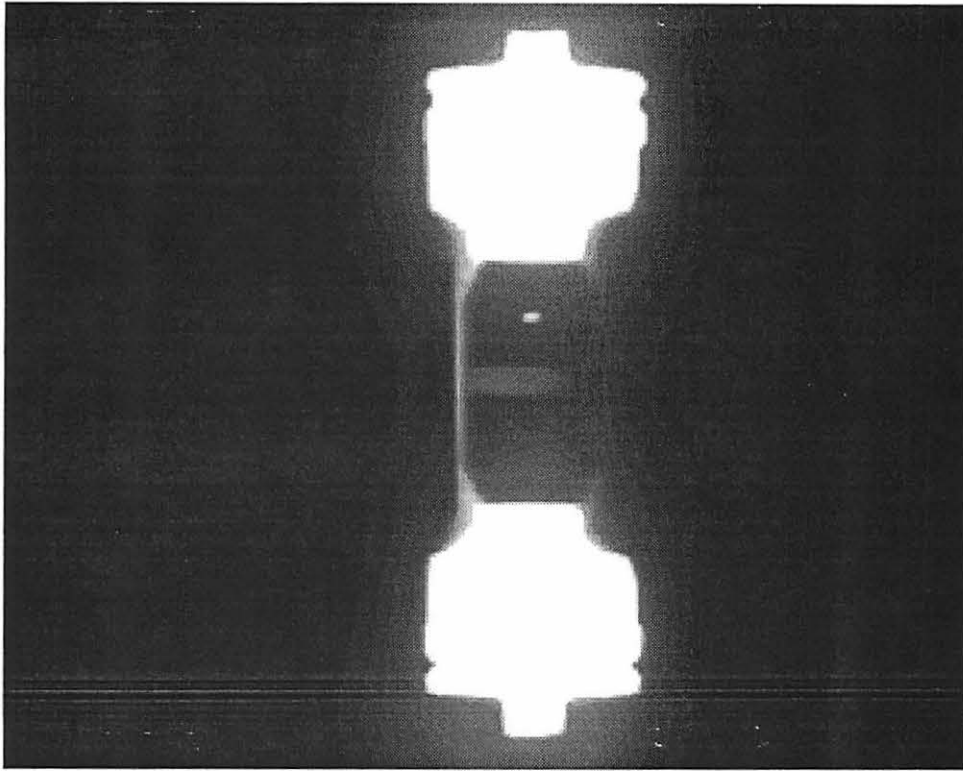


Figure 4.1 Image of air conditioner compressor part taken at an illumination of 80% of maximum.

Figure 4.3 shows the same part's radio-graph digitized under an illumination of 60% of maximum light intensity. This image shows that all densities less than 1.75 results in a gray scale of 255 and all pixels having an image density of greater than 2.55 results in a gray-scale of 0.

Figure 4.4 shows the same part's radio-graph digitized under an illumination of 55% of maximum light intensity. This image shows that all densities less than 2.25 results in a gray scale of 255 and all pixels having an image density of greater than 3.0 results in a gray-scale of 0.

These four images, taken at the same orientation of the x-ray radio-graph and under the given illuminations, was fed to the algorithm which processed the images resulting in a *compositized* image, shown in Figure 4.5. Though, the display system used was as such that it accepted only an 8-bit image, this *compositized* image does not display in-

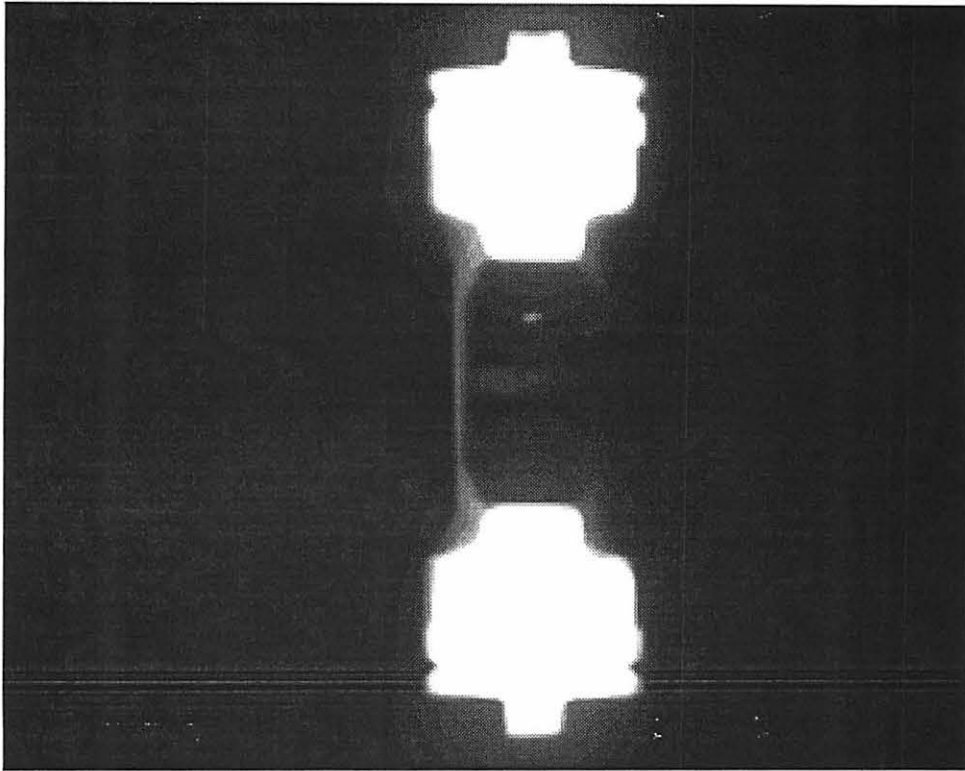


Figure 4.2 Image of air conditioner compressor part taken at an illumination of 70% of maximum.

formation in a manner in which the inherent material defects are evident to the observer.

Evident from the *composite* image, is the fact that the visual information available is limited, and, one is not able to clearly see and make out the flaws present. Since we developed a method to view a specified range of gray-scales (and hence, image densities), we were able to select a minimum and a maximum and scale this range to the available gray-scales, resulting in the images of Figures 4.6, 4.7, 4.8, and 4.9.

These images were for a minimum-maximum gray-scale settings of 2389-3893 (Figure 4.6), 3072-4160 (Figure 4.7), 5415-7205 (Figure 4.8) and 7214-8192 (Figure 4.9).

Although these settings of the minimum and maximum gray-scales can be done as a continuous process, thereby changing the range of view incrementally, presented here is only four of those image range settings.

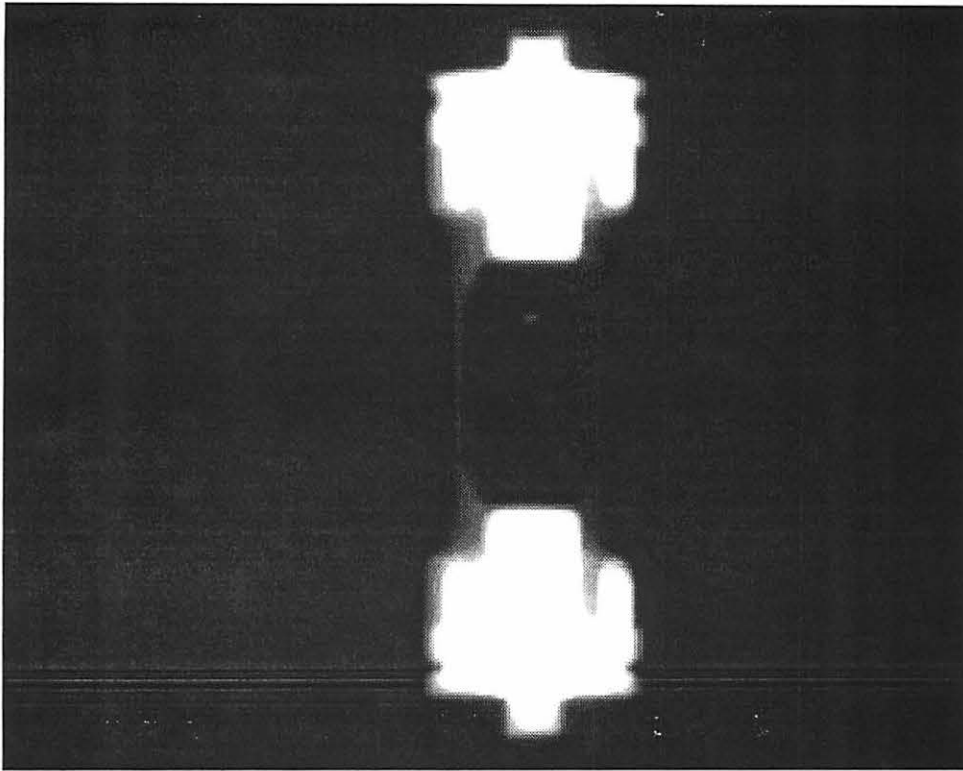


Figure 4.3 Image of air conditioner compressor part taken at an illumination of 60% of maximum.

Weld Thickness Measurements

One of the applications of the system developed is the measurement of the weld penetration depth, in incomplete or Lack Of Penetration (LOI) instances. A field run on a automobile transmission casing welding was conducted to measure quantitatively the depth of penetration.

Figure 4.10 shows the typical profile of a welding. Here, it is necessary that the thickness $b - c$ be measured, which will give the thickness of the air gap in the welding. We were able to measure the thickness of the penetration to within 5% accuracy.

With a radiograph of a calibration sample made of similar material as this casing, and its thickness known, we can obtain a plot of the thickness versus density. Using this plot (shown in Figure 4.11) we can obtain the sample's thickness at various points

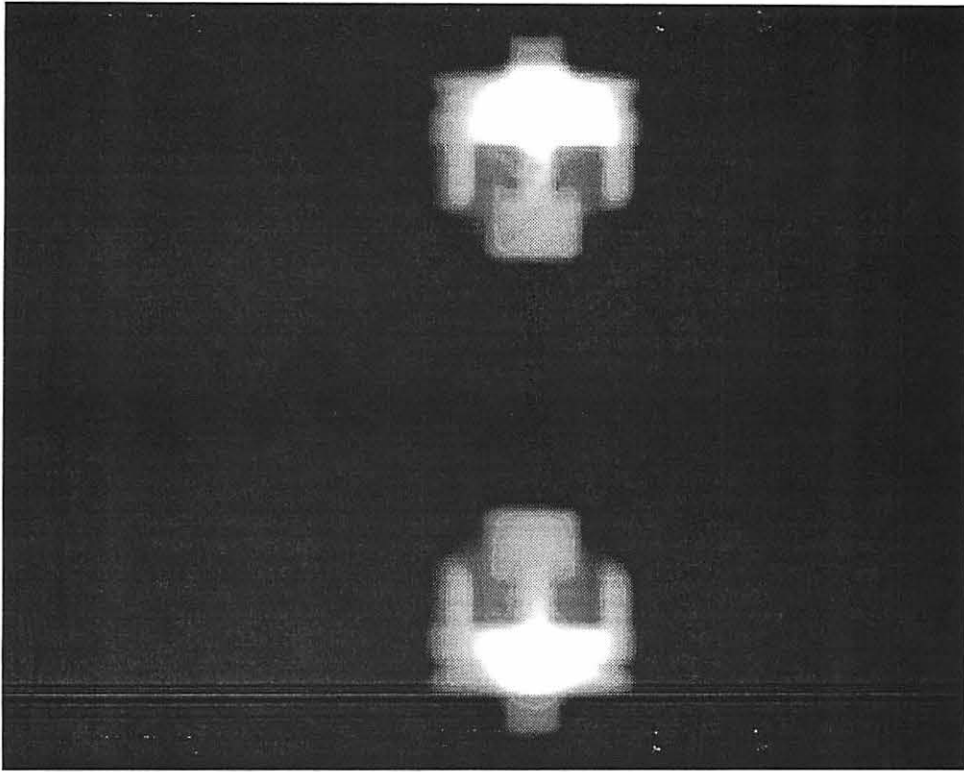


Figure 4.4 Image of air conditioner compressor part taken at an illumination of 55% of maximum.

of interest (*a*, *b*, and *c*). Further, in order to emphasize the region of interest, we set the minimum and maximum gray-scales at 3362 and 5272 respectively.

Figure 4.12 shows the standard sample's *compositized* image and Figure 4.13 shows the Eaton transmission casing's *compositized* image. Both these images are for a minimum-maximum gray-scale setting of 3362 and 5272 respectively. It can be seen that the dark line in the middle of the welding is the air gap in the welding.

EPRI's Proposed Standard

Figure 4.14 shows the composite image of the radiograph obtained from EPRI before it was accepted as a standard radiograph. The outcome of a beta testing of this standard using the system developed, resulted in a suggestion, which was later incorporated. As can be seen, the optical density step size of the calibration strip in this radiograph is

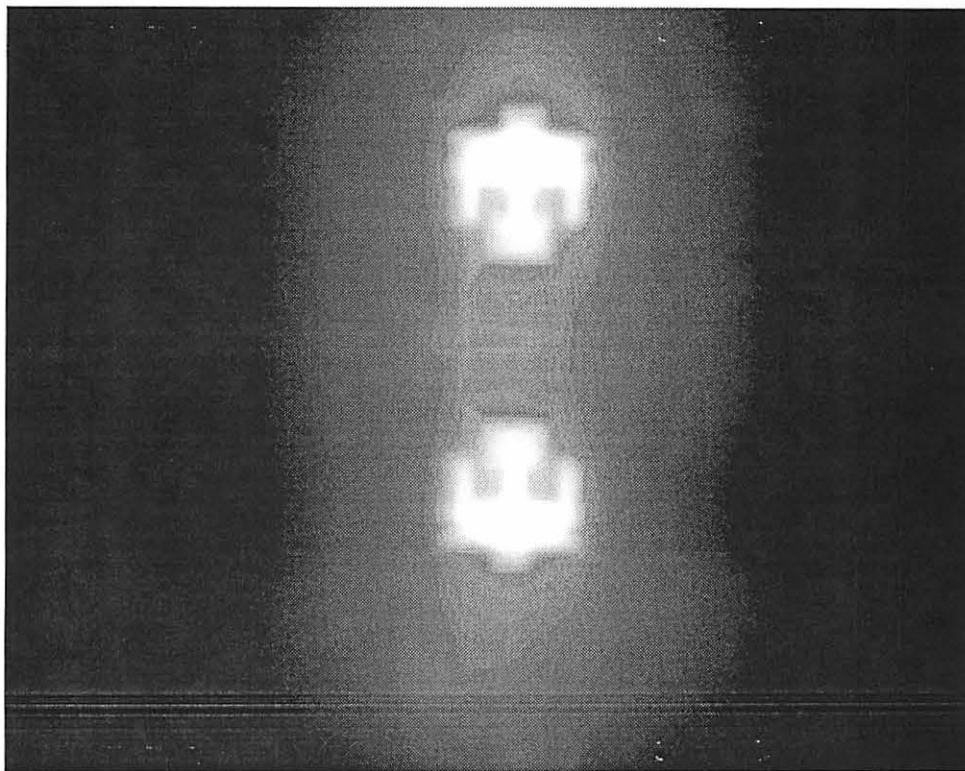


Figure 4.5 *Compositized* image, resulting from the image enhancement process.

high, and as a result of which, there are not sufficient data points that can be used to calibrate a system. Since such standards were seldom tested on such low-end systems, such principal correctional suggestions were not made by other high-end film digitization methods. The minimum contrast required to be resolved in this standard was a $\Delta D = 0.01$ over a total density range of 4.0. The system developed, was able to resolve these densities. The resolution requirements for the EPRI standard was 70 micron pixel sizes. This was achieved by narrowing the field of view to 1.8×1.8 inches.

Digitized ASTM Standard Radiographs

Figures 4.15 and 4.16 show the digitized images of the *E 446*, reference radiographs for the steel castings taken at medium voltage (nominal 250 KVp) x-rays. These radiographs were obtained from ASTM, showing the shrinkage porosity in steel castings, and, sand

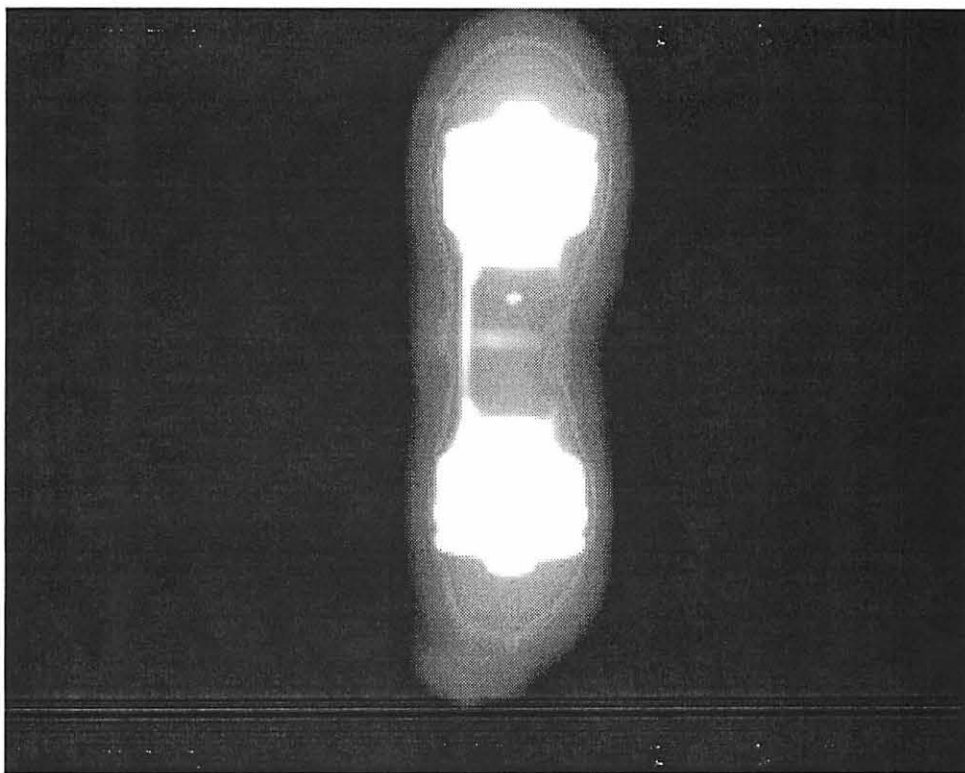


Figure 4.6 *Composite image with gray-scale window of 2389-3893.*

and slag inclusions respectively, and digitized using the developed system. It can be seen that the amount of detail captured in these images is high, which is a direct consequence of the system and algorithm used to digitize and enhance these images.

Another standard radiograph used to test the resolution limits of the system developed (to compare it with the ability of the human eye to differentiate variations in optical densities and resolution, from a direct viewing of a radiograph), was the penetrameter measurements. Figure 4.17 shows the digitized radiograph of a penetrameter on 1 inch of Aluminum at 120 kV without any filter. The sample was created by clamping 15 sheets of 0.061 inch 2024 Aluminum together for a total thickness of 0.915 inch. Penetrators were taped to the surface. It can be seen that the composite image (Figure 4.17) does not show as much detail as that when seen from the radiograph directly. But when the minimum-maximum settings of the composite image is set to 2657-3459, the

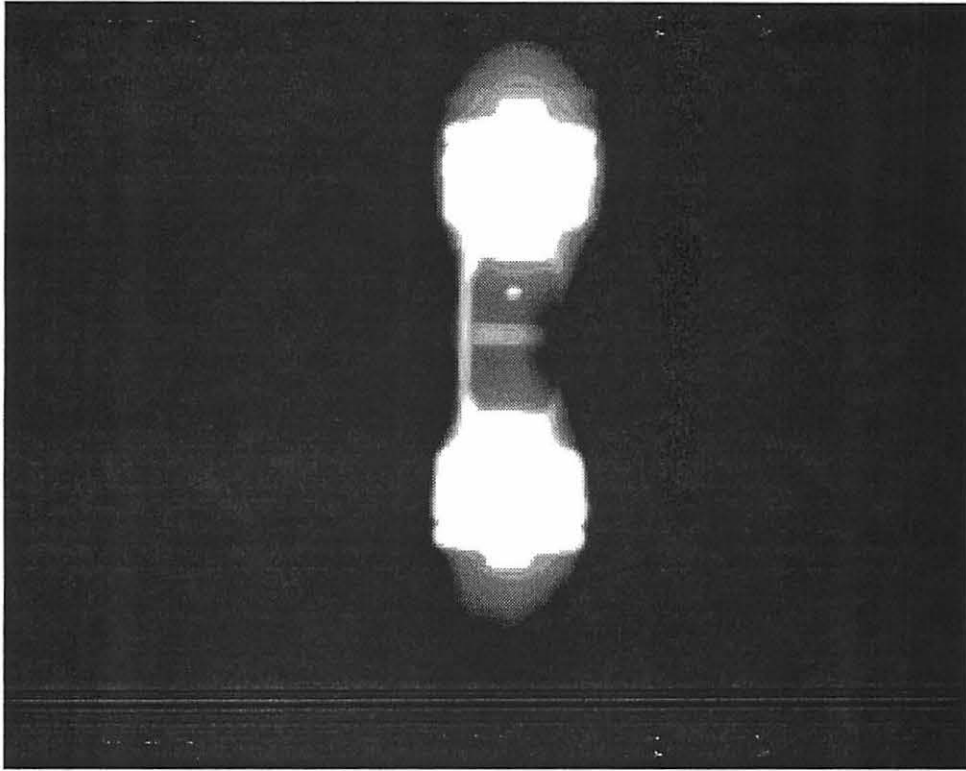


Figure 4.7 *Composite image with gray-scale window of 3072-4160.*

resultant image is shown in Figure 4.18. This figure shows the 4T hole in the penetrator for the 11 sample, which is as far that the eye can perceive from the x-ray radiograph directly. This is an affirmation of the fact that, we were able to store as much information as we can get viewing the radiograph directly. Hence the digitization process has not lost much of the information available.

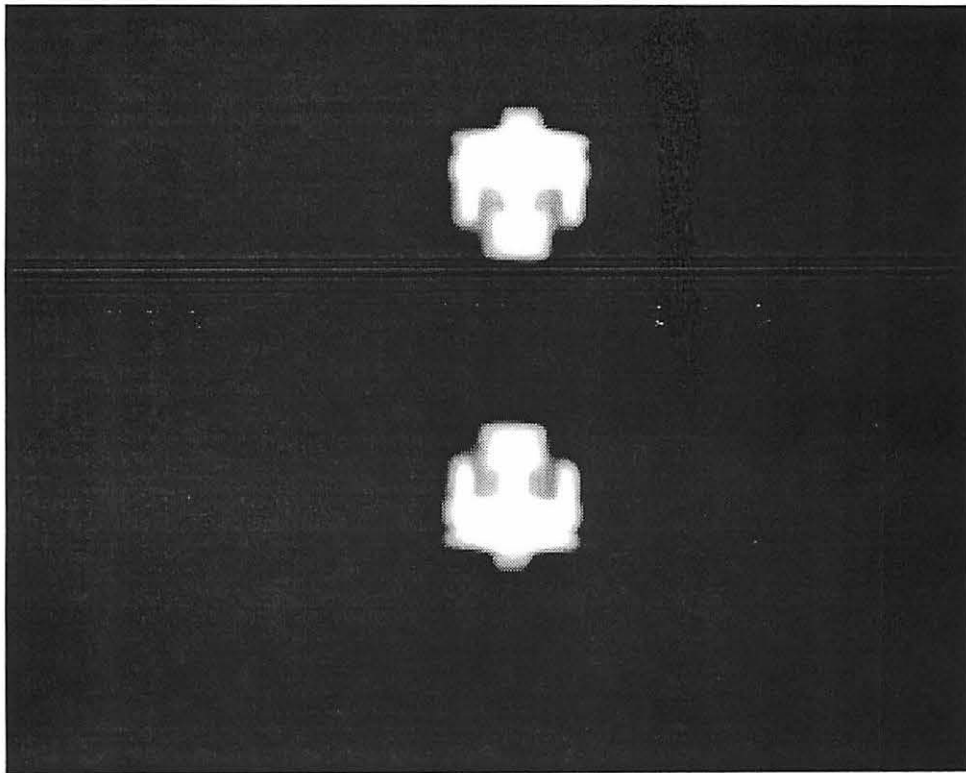


Figure 4.8 *Composite image with gray-scale window of 5415-7205.*

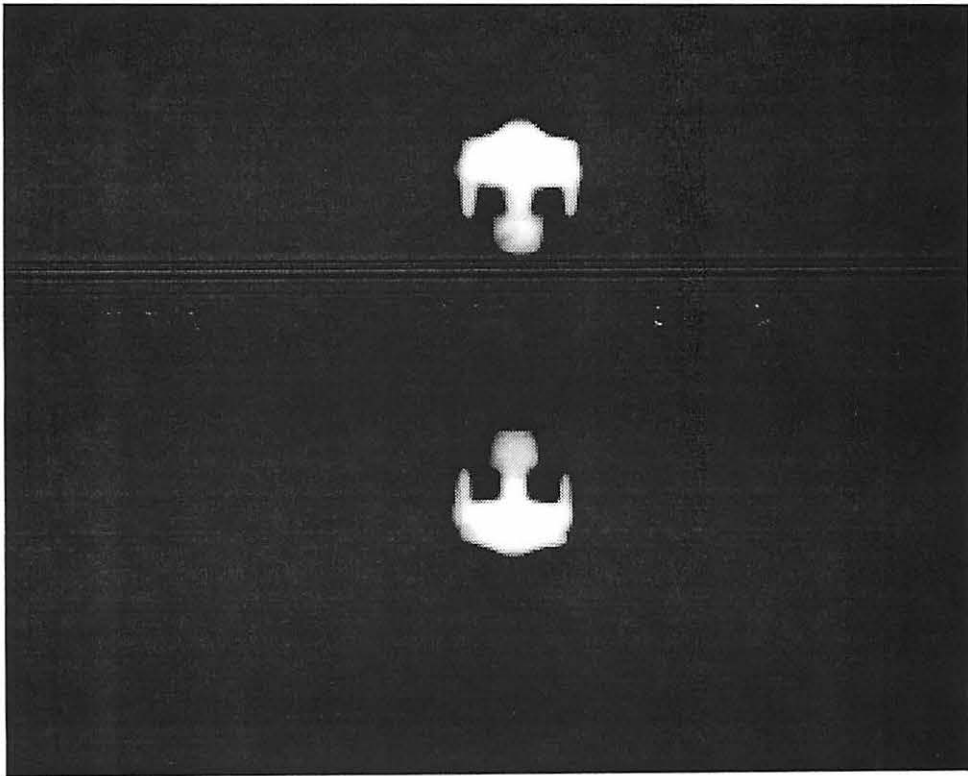


Figure 4.9 *Composite* image with gray-scale window of 7214-8192.

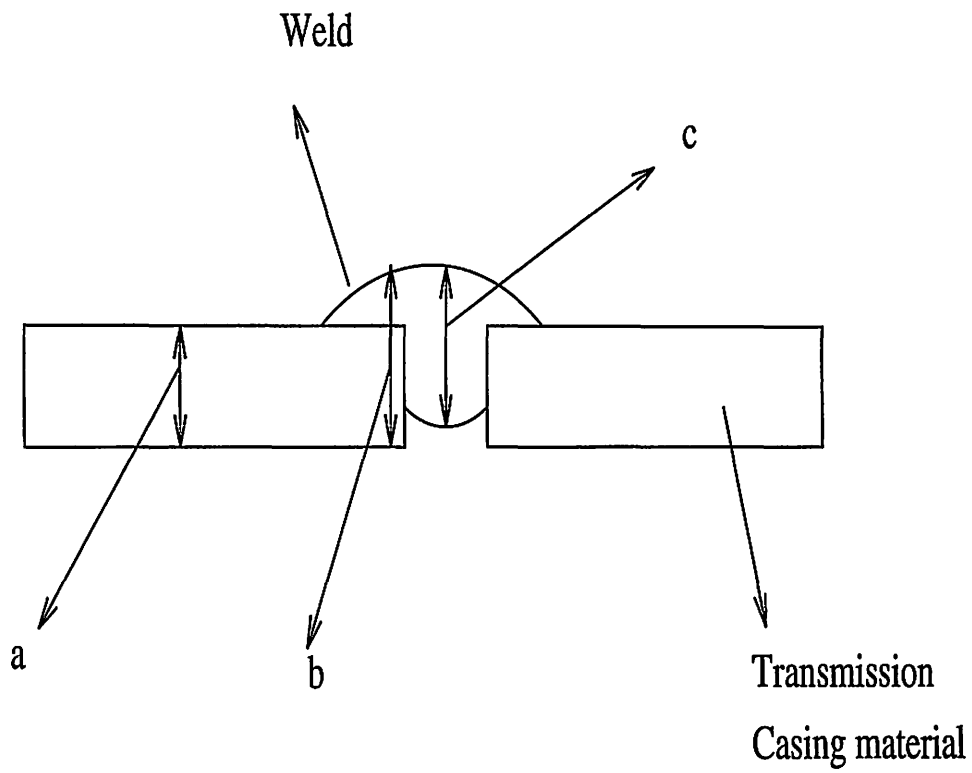


Figure 4.10 Welding profile of a transmission casing.

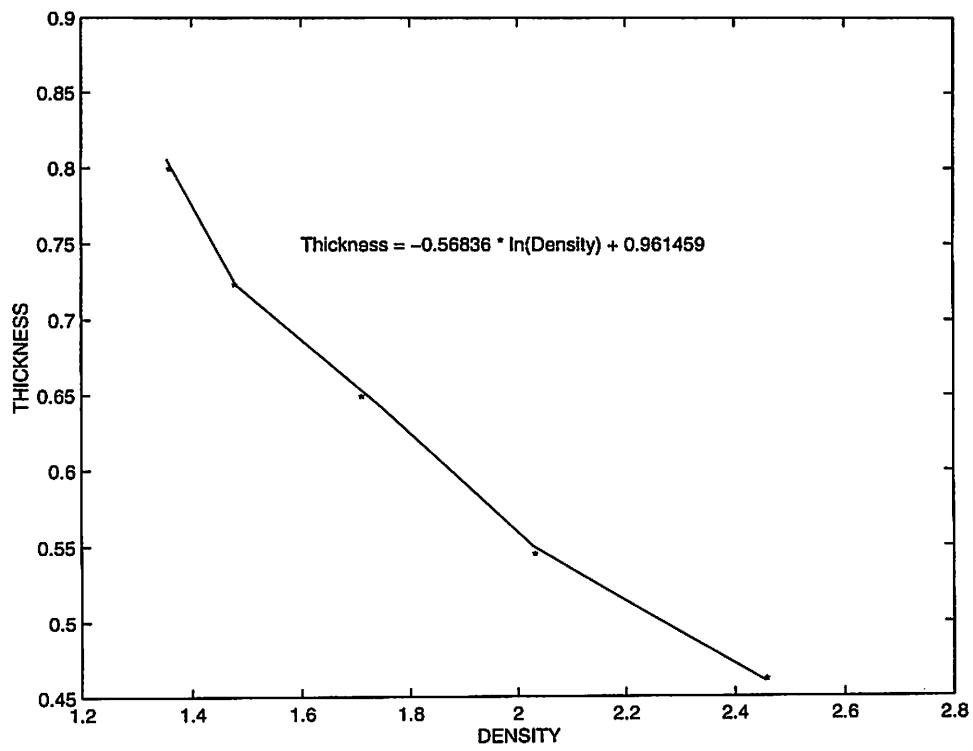


Figure 4.11 Thickness versus gray-scale calibration.

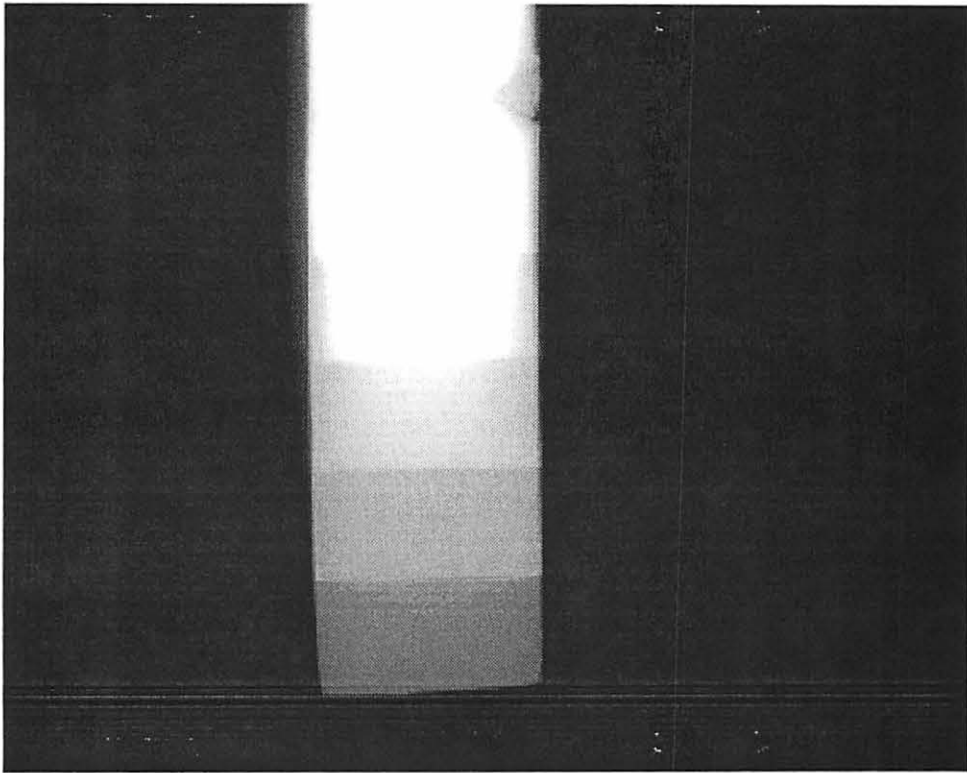


Figure 4.12 Standard sample image.

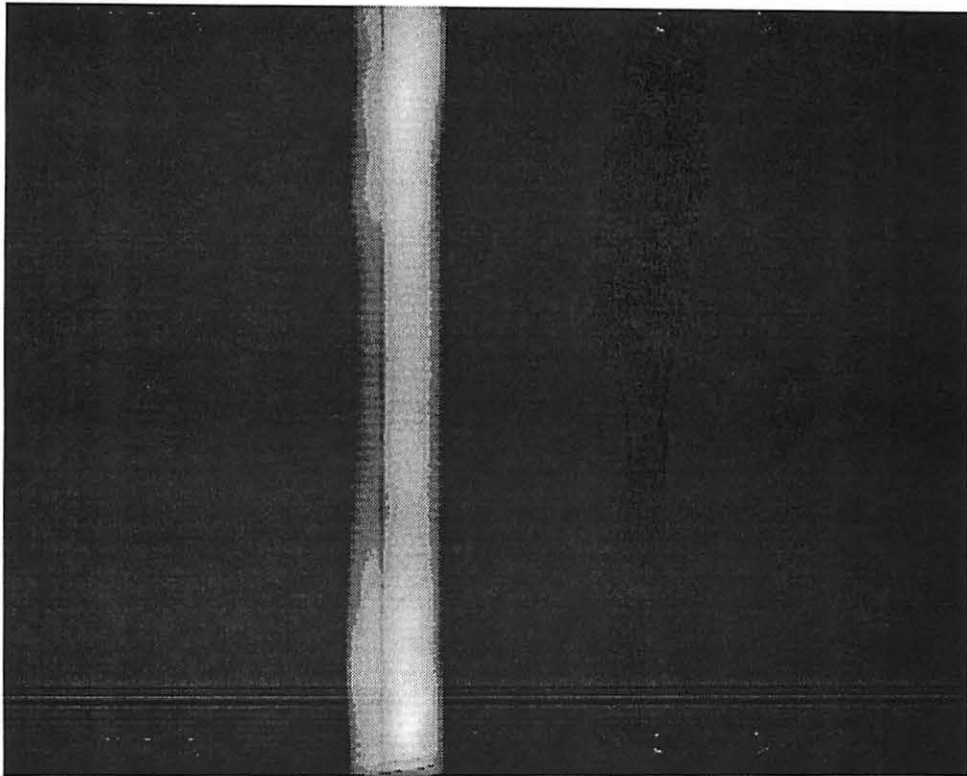


Figure 4.13 Eaton transmission casing's image.

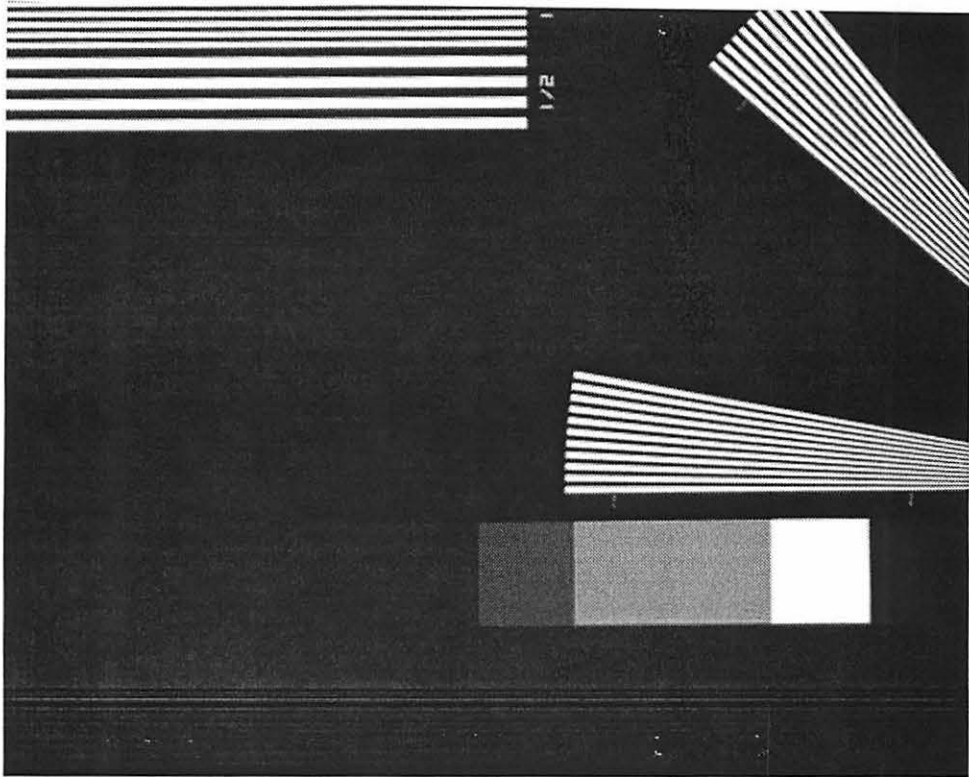


Figure 4.14 EPRI's proposed standard radiograph, under test.

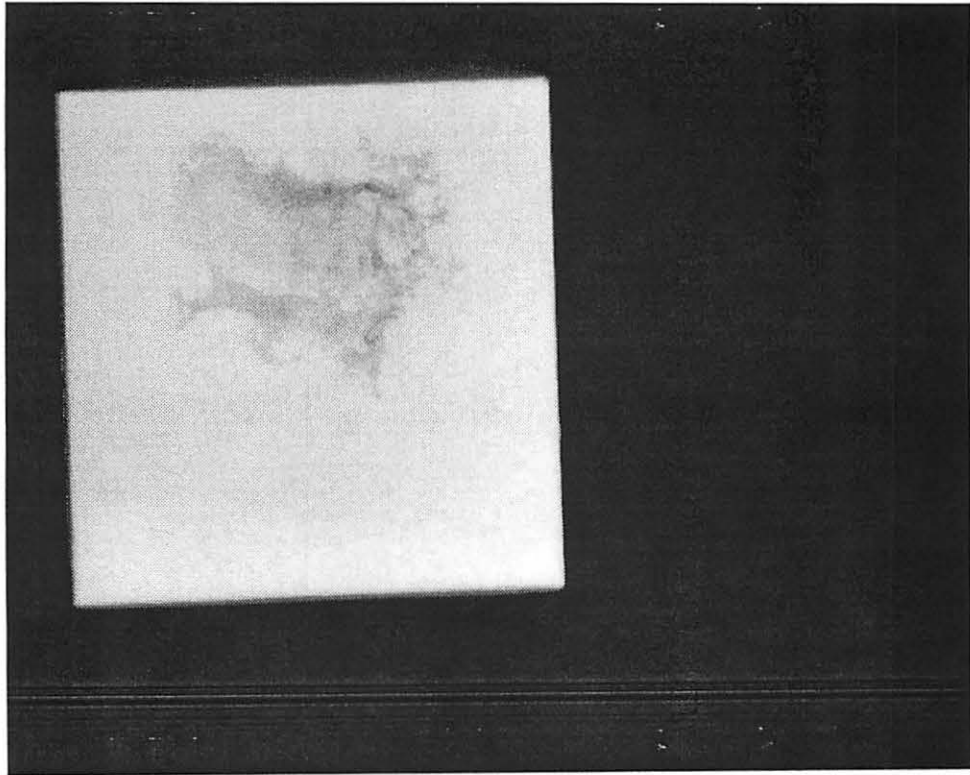


Figure 4.15 Image of ASTM's standard radiograph showing shrinkage porosity.

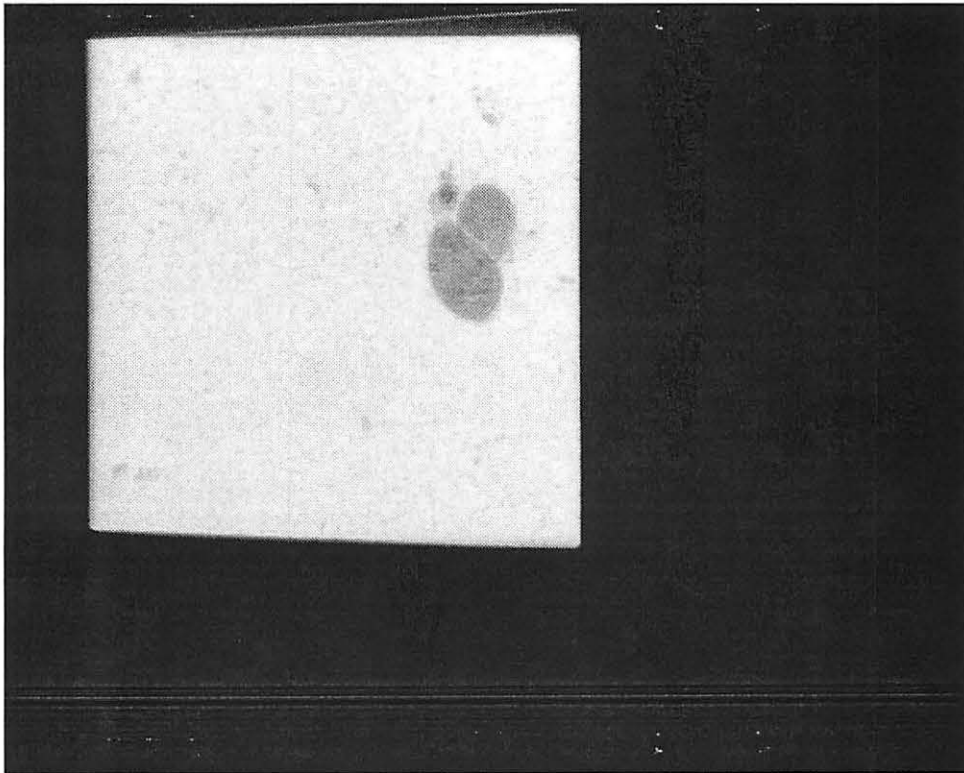


Figure 4.16 Image of ASTM's standard radiograph showing sand and slag inclusions.

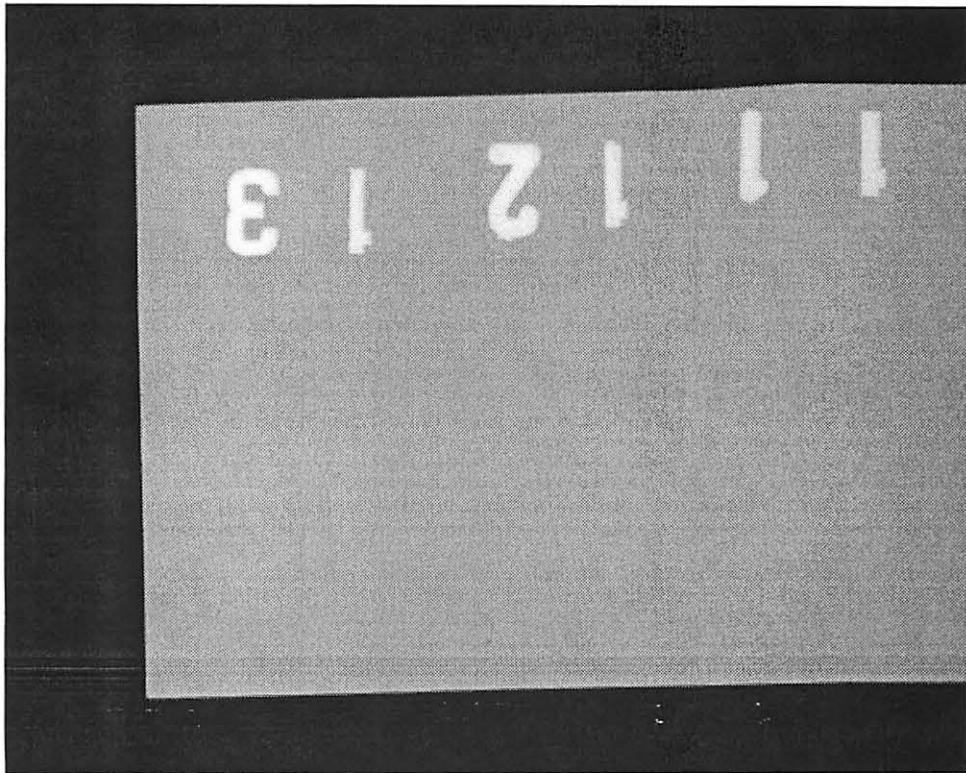


Figure 4.17 Composite image of penetrometer radiograph.

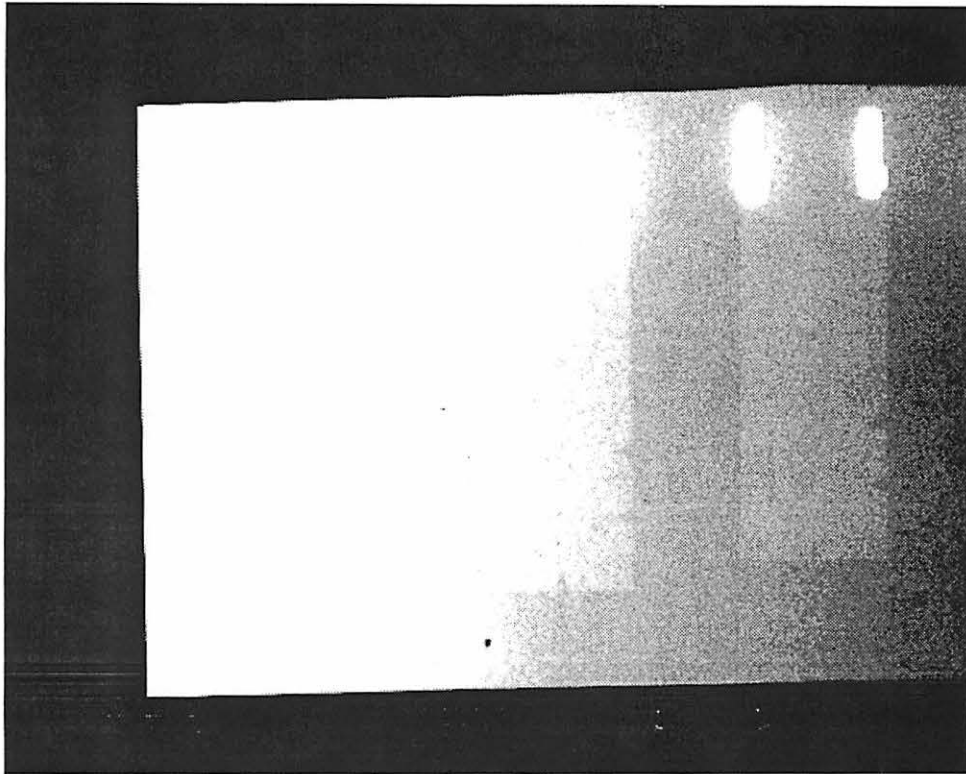


Figure 4.18 Composite image of penetrometer radiograph with min-max window of 2657-3459.

5 CONCLUSIONS AND FUTURE WORK

There are two distinct facets of visual x-ray flaw detection. One is to be able to acquire and digitize this x-ray radiographic image in such a way as to obtain enough information, which will aid in flaw detection. The other aspect is the ability to represent such images which will facilitate the investigator to pin-point specific areas found defective.

The first objective can be achieved by opting for high-end image digitizers, which invariably are turning out to be laser based, which can be very prohibitive in terms of cost. Further, such digitizers, though only have a static range of densities that they are capable of handling, are used in most medical imaging applications. We, however wanted a more cost effective system, aiding in material inspection, which will give the same information as their medical counterparts.

The second objective is a limitation of both, the display systems available and also the natural limitation of the human eye. In order to get around this problem would mean devising novel display systems and providing the investigator with tools to be able to view smaller dynamic ranges of the image and at the same time be able to span through the entire range of densities. This has the effect of amplifying a small window to fit the entire display range, thereby enabling him to discern more easily the compositional variations in the radiograph.

In order to utilize existing the x-ray imaging system available, we decided to obtain radiographs and then digitize them, resulting in a two step process. An 8-bit digitizer was used to obtain individual images of the radiographs. We were successful in devising

an algorithm that would be able to obtain a single image which contained information about the entire range of densities, even if such information was not available in a single image to start with. This in effect was like using a very high-end digitizer which had close to 16-bits. We also had to design a light box which could be program controlled, as it was necessary to change the illumination intensity at various stages of the algorithm. The first objective of extracting as much information as possible from the radiograph was thus achieved.

The format for storing such an x-ray image was the one conventionally followed here. It is a simple array of 307200 pixels (derived from 640×480) with each pixel an unsigned short integer (implying that it is a 16 bit quantity). This was to be able to store information about image which could theoretically have grayscales ranging from 0 to 2^{16} . This resulted in no loss of information due to the digitization process.

The system's user interface had the capability of dynamically varying the range of densities (or grayscales) of interest, and then displaying the resulting image on the TV monitor. The implemented algorithm was inherently to overcome the second bottleneck mentioned earlier.

These techniques worked up to expectations when we digitized radiographs taken from typical industrial parts that included aluminum castings. Erstwhile digital images had not given information about the presence of flaws which were not detectable due to such minute changes in the densities that they were not being represented in the digital image. A 12-bit digitizer was also used to see the difference between the quality of image available. 12 bits were not sufficient enough to obtain enough information regarding the density variations in a single image.

Future Work

A system for obtaining an accurate calibration between the density-grayscale, relationship at a given illumination intensity, was found to be very difficult. Standard calibration radiographs obtained from the industry did not have enough density resolution to provide us with enough data points which may result in a better calibration. Better standards should be devised which could accurately predict the densities from grayscales and vice-versa.

This is an important step in moving, more from a qualitative inspection technique, to providing accurate quantitative information.

Making this system a real-time system is both the logical next step as well as an important stage in creating a wholesome x-ray NDE set-up. This should involve using film-less radiography, where the object of obtaining a radiograph and then processing it to obtain digital image could be done away with, and instead the digital information from the image intensifier forms the basis for further processing.

Most other image processing techniques which were discussed earlier can be implemented, which might be useful in obtaining and manipulating the digital image data.

REFERENCES

- [1] R. Halmshaw. *Non-Destructive Testing*. London, England: Edward Arnold; 1987.
- [2] Elizabeth M. Siwek. *Application of the X-ray Measurement Model to Image Processing of X-ray Radiographs*. M.S. Thesis, Iowa State University; 1994.
- [3] Eastman Kodak Co. *Radiography in Modern Industry*, 4th ed. Rochester, NY; 1980.
- [4] H. K. Huang. *Elements of Digital Radiography*, Englewood Cliffs, New Jersey: Prentice Hall; 1987.
- [5] Joseph N. Gray and Terence Jensen. *Review of Progress in QNDE Conference Proceedings*, Plenum Press, New York: Vol. 15A, 1996: 441-448.
- [6] Stephen Wong, Loren Zaremba, David Gooden and H. K. Huang. Radiologic Image Compression. *Proceedings of the IEEE*, Vol. 83, No. 2, February, 1995.
- [7] S. C. Lo, R. K. Tiara, N. J. Hankovich and H. K. Huang. Performance Characteristics of a Laser Scanner and Laser Printer System for Radiological Imaging. *Computerised Radiology*, Vol. 10, No. 5, 1986: 227-237.
- [8] *Technical Manual for DVC Cameras*, Manual Number 86-001-01, DVC Company San Diego, November 1995.
- [9] Anil K. Jain. *Fundamentals of Digital Image Processing*, Englewood Cliffs, New Jersey: Prentice Hall; 1989.